Cbs overdosage is necessary and sufficient to induce cognitive phenotypes in mouse models of Down syndrome and interacts genetically with Dyrk1a

Damien Marechal, Véronique Brault, Alice Leon, Dehren Martin, Patricia Pereira, Nadège Loaëc, Marie-Christine Birling, Gaëlle Friocourt, Marc Blondel, Yann Herault

Human Molecular Genetics, 2019, Vol. 00, No. 00 1–17

doi: 10.1093/hmg/ddy447
Advance Access Publication Date: 10 January 2019
General Article

GENERAL ARTICLE

Cbs overdosage is necessary and sufficient to induce cognitive phenotypes in mouse models of Down syndrome and interacts genetically with *Dyrk1a*

Damien Marechal[1,2,3,4], Véronique Brault[1,2,3,4], Alice Leon[5], Dehren Martin[1,2,3,4], Patricia Lopes Pereira[6], Nadege Loaëc[5], Marie-Christine Birling[7], Gaelle Friocourt[5,†], Marc Blondel[5,†] and Yann Herault[1,2,3,4,7,*]

[1]Institut de Génétique et de Biologie Moléculaire et Cellulaire, Illkirch, 1 rue Laurent Fries, 67404 Illkirch, France, [2]Centre National de la Recherche Scientifique, UMR7104, 67404 Illkirch, France, [3]Institut National de la Santé et de la Recherche Médicale, U1258, 67404 Illkirch, France, [4]Université de Strasbourg, 67404 Illkirch, France, [5]Inserm UMR 1078, Université de Bretagne Occidentale, Faculté de Médecine et des Sciences de la Santé, Etablissement Français du Sang (EFS) Bretagne, CHRU Brest, Hôpital Morvan, Laboratoire de Génétique Moléculaire, 29200 Brest, France, [6]Transgenese et Archivage Animaux Modèles, TAAM, CNRS, UPS44, 3B Rue de la Férollerie 45071 Orléans, France, [7]CELPHEDIA, PHENOMIN, Institut Clinique de la Souris, ICS, 1 Rue Laurent Fries, 67404 Illkirch, France

*To whom correspondence should be addressed at: Institut de Génétique et de Biologie Moléculaire et Cellulaire, 1 Rue Laurent Fries, 67404 Illkirch, France. Tel: +33 388 65 5715; Fax: +33 388 65 3201; Email: herault@igbmc.fr

Abstract

Identifying dosage-sensitive genes is a key to understand the mechanisms underlying intellectual disability in Down syndrome (DS). The Dp(17Abcg1-Cbs)1Yah DS mouse model (Dp1Yah) shows cognitive phenotypes that need to be investigated to identify the main genetic driver. Here, we report that three copies of the cystathionine-beta-synthase gene (*Cbs*) in the Dp1Yah mice are necessary to observe a deficit in the novel object recognition (NOR) paradigm. Moreover, the overexpression of *Cbs* alone is sufficient to induce deficits in the NOR test. Accordingly, overexpressing human *CBS* specifically in Camk2a-expressing neurons leads to impaired objects discrimination. Altogether, this shows that *Cbs* overdosage is involved in DS learning and memory phenotypes. To go further, we identified compounds that interfere with the phenotypical consequence of CBS overdosage in yeast. Pharmacological intervention in Tg(*CBS*) mice with one selected compound restored memory in the NOR test. In addition, using a genetic approach, we demonstrated an epistatic interaction between *Cbs* and *Dyrk1a*, another human chromosome 21-located gene (which encodes the dual-specificity tyrosine phosphorylation-regulated kinase 1a) and an already known target for DS therapeutic intervention. Further analysis using proteomic approaches highlighted several molecular pathways, including synaptic transmission,

[†]Both authors contributed equally.

Received: October 13, 2018. **Revised:** December 17, 2018. **Accepted:** December 18, 2018

cell projection morphogenesis and actin cytoskeleton, that are affected by DYRK1A and CBS overexpression. Overall, we demonstrated that CBS overdosage underpins the DS-related recognition memory deficit and that both *CBS* and *DYRK1A* interact to control accurate memory processes in DS. In addition, our study establishes CBS as an intervention point for treating intellectual deficiencies linked to DS.

Significant statement

Here, we investigated a region homologous to Hsa21 and located on mouse chromosome 17. We demonstrated, using three independent genetic approaches, that the overdosage of the cystathionine-beta-synthase gene (*Cbs*) gene encoded in the segment is necessary and sufficient to induce a deficit in the novel object recognition (NOR) test.

In addition, we identified compounds that interfere with the phenotypical consequence of CBS overdosage in yeast and in mouse transgenic lines. Then we analysed the relation between CBS overdosage and the consequence of DYRK1a overexpression, a driver of Down syndrome (DS) cognitive phenotypes found in another region homologous to Hsa21. We demonstrated that an epistatic interaction exists between *Cbs* and *Dyrk1a* and that it affects different pathways, including synaptic transmission, cell projection morphogenesis and actin cytoskeleton.

Introduction

Down Syndrome (DS) is the most common aneuploidy observed in human. The presence of an extra copy of the human chromosome 21 (Hsa21, Hsa for *Homo sapiens*) is associated with intellectual disabilities and several specific morphological and physiological features. Phenotypic mapping in human bearing partial duplication highlighted the contribution of several regions of the Hsa21 to DS features (1,2). Additional information was collected from trisomic and monosomic mouse models to detect genomic regions sensitive to dosage and able to induce impairments in behaviour and other DS-related traits (3–11). Most of the efforts focused on the region homologous to the Hsa21 located on mouse chromosome 16 (Mmu16, *Mmu for Mus musculus*), highlighting the contribution of overdosage of the amyloid precursor protein (12), the glutamate receptor, ionotropic, kainate 1 (*Grik1*) or the dual-specificity tyrosine phosphorylation-regulated kinase 1a *(Dyrk1a)* (13,14) to DS cognitive defects. DYRK1A is currently the main target for therapeutic intervention with the identification of a few compounds inhibiting its kinase activity and improving mainly cognition in DS mouse models (15–20). However, models carrying trisomy of the region of Mmu17 homologous to the Hsa21 also showed learning and memory defects (21,22) and appeared to have a major impact on DS phenotypes in mouse models (23). The Dp(17*Abcg1-Cbs*)1Yah (called here Dp1Yah) mice are trisomic for 12 protein-encoding genes including three members of the trefoil factor families (*Tff1-3*), *Tmprss3*, *Ubash3a*, *Rsph1*, *Slc37a1*, *Pknox1, Pde9a, Ndufv3, Wdr4* and *Cbs*. The region also encompasses six non-coding genes: *Gm25447* (rRNA), *Gm15318* (antisense lncRNA), *Gm8437* (unclassified), *Gm9902* (unclassified), *4833413E03Rik* (lincRNA) and *Gm24970* (miRNA). The Dp1Yah mice are defective in the novel object recognition (NOR) test and show long-lasting *in vivo* long-term potentiation (LTP) in the hippocampus while the corresponding monosomy in Ms2Yah mice (in which *Abcg1* and *U2af1* are deleted), induces defects in social discrimination with increased *in vivo* LTP (24). Interestingly, as observed in the rotarod test, the locomotor phenotype of the Tc1 transchromosomic mouse model carrying an almost complete Hsa21 is rescued when the *Abcg1-Cbs* region is returned to two copies in Tc1/Ms2Yah mice (25). Similarly, the trisomy of a larger overlapping segment on Mmu17 from *Abcg1* to *Rrp1b* induces an increased LTP as compared with controls in the Dp(17)Yey model (22) and was shown to genetically interact with the trisomy of the *Lipi-Zbtb21* interval. More specifically, the trisomy of both the *Abcg1-Rrp1b* region and the *Cbr1-Fam3b* region was detrimental for learning and memory in the Morris water maze and for LTP in DS mouse models (23).

Among the 11 trisomic genes in the Dp1Yah model, the *Cbs*, encodes a pyridoxal phosphate-dependent enzyme converting homocysteine to cystathionine. This first step of the transsulfuration pathway removes homocysteine from the methionine cycle thereby also affecting the folate and the methylation pathways, while contributing to the cysteine cycle. Of note, in human, homozygous loss-of-function mutations in *CBS* are associated with homocystinuria (OMIN236200), a metabolic condition with intellectual disability. CBS is also the major enzyme catalysing the production of H_2S from L-cysteine (26) or from the condensation of homocysteine with cysteine (27). H_2S is now considered a major gasotransmitter in the brain (28) and interferes with synaptic transmission. Considering the up-regulated expression of CBS in several brain regions of the Dp1Yah model and its impact on intellectual disability, we decided to focus on *Cbs* and decipher the role of CBS in DS cognitive phenotypes. To this end, we generated and characterized constitutive and conditional changes in *Cbs* dosage in the nervous system of various mouse models. In addition, we identified pharmacological drugs able to counteract the phenotypical consequence of CBS overexpression, in particular behavioural impairments, and finally further analysed molecular changes induced by *Cbs* overdosage to understand the mechanisms perturbed in DS models.

Materials and Methods

Ethics statement, mouse lines and genotyping

Animal experiments were approved by the Com'Eth N°17 (project file: 2012-069) and accredited by the French Ministry for Superior Education and Research and in accordance with the Directive of the European Parliament: 2010/63/EU, revising/replacing Directive 86/609/EEC and with French Law (Decree n° 2013-118 01 and its supporting annexes entered into legislation 01 February 2013) relative with the protection of animals used in scientific experimentation. YH was granted the accreditation 67-369 to perform the reported experiments in the animal facility (Agreement C67-218-40). For all these tests, mice were kept in specific pathogen-free conditions with free access to food and water. The light cycle was controlled as 12 h light and 12 h dark (lights on at 7 AM). All the behavioural tests were performed between 9:00 AM and 4:00 PM.

Several mouse lines were used to decipher the influence of *Cbs* dosage changes: the trisomic mouse model, Dp(17Abcg1-

Cbs)1Yah, named here Dp1Yah, carries a segmental duplication of the *Abcg1-Cbs* region of the Mmu17 (21) kept on the C57BL/6 J genetic background with continuous backcross during all the study (N > 7 generations); the inactivated allele of C57BL/6 J.*Cbs*^{tm1Unc} (29); and the PAC transgenic line Tg(*CBS*)11181Eri [named here Tg(*CBS*)], originally identified as 60.4P102D1 (30) and backcrossed on C57BL/6J for more than seven generations. We designed, generated and selected the transgenic mouse line Tg(*Prp-gfp-CBS*)95-157ICS, named here Tg(*Prp-gfp-CBS*), to overexpress the human *CBS* cDNA from the murine prion promoter region (containing a 8477 bp region upstream of the ATG of the murine prion gene, i.e. 6170 bp promoter region, exon 1, intron 1 and beginning of exon 2) after the excision of a loxP-*gfp-loxP* interrupting cassette (Fig. 3A). The transgenic mouse line was generated on the C57BL/6N genetic background. We used the transgenic Tg(Camk2a-cre)4Gsc mouse line (31), named here Tg(*Camk2a-cre*), as a glutamatergic neuron-specific Cre driver. The line was further bred on C57BL/6J for more than seven generations. When the Tg(Camk2-Cre)/0 × Tg(Prp-gfp-CBS)/0 cross was done, the genetic background of the cohorts was estimated to be around C57BL6 J(57%)/N(43%). The Dyrk1a BAC transgenic mouse line, named here Tg(*Dyrk1a*), was previously generated in our laboratory (32,33) and their study was performed on animals with more than seven generations of backcross on the C57BL/6J genetic background. The cohorts for the Tg(Dyrk1a) and Dp1Yah were produced on the B6J genetic background (estimated at 98.8%). Genotype identification was performed on genomic DNA isolated from tail biopsies with specific PCR (Supplementary Material, Table S1).

Behavioural analysis

The number of animals required for behavioural analysis was estimated according to similar experiments we previously performed in DS mouse models (5,21,25). All the mice used in the study were males and the controls were littermates. To investigate the role of *Cbs* in the Dp1Yah cognitive phenotypes, we generated two independent cohorts [cohort 1 (C1): wild-type (wt) littermates n = 11; *Cbs*$^{tm1Unc/+}$, n = 8; Dp1Yah, n = 8; Dp1Yah/*Cbs*^{tm1Unc}, n = 11; and cohort 2 (C2): wt littermates n = 18; *Cbs*$^{tm1Unc/+}$, n = 15; Dp1Yah, n = 15; Dp1Yah/*Cbs*^{tm1Unc}, n = 10]. All cohorts were evaluated in several tests in adult mice, the open field (C1: 33 weeks, C2: 14–16 weeks), NOR (C1: 33 weeks, C2:14–16 weeks), Y-maze (C2: 15–19 weeks) and rotarod (C2: 25–28 weeks of age).

Wt littermates (n = 13) and Tg(CBS)/0 (n = 17) hemizygotes were tested for circadian actimetry (14 weeks), Y-Maze (16 weeks), open field (17 weeks) and NOR (17 weeks). We added an additional group of wt (n = 9) and Tg(CBS)/0 (n = 10) to validate the results obtained in the NOR test for which animals were tested at the same age (17 weeks). A cohort with four genotypes [wt (n = 13), Tg(Camk2-Cre)/0 (n = 11), Tg(*Prp-gfp-CBS*)/0 (n = 12) and Tg(Camk2-Cre)/0, Tg(*Prp-gfp-CBS*)/0 (n = 14)] was evaluated through the same behavioural tests: rotarod (14 weeks), Y-maze (16 weeks), open field (19–20 weeks) and NOR (19–20 weeks). A total of 14 wt, 15 Tg(*Dyrk1a*), 13 Dp1Yah and 13 Dp1Yah/Tg(*Dyrk1a*) mutant mice were evaluated for the open field exploration (11–12 weeks), NOR test (11–12 weeks) and Y-maze (13 weeks). A second independent cohort with 11 wt, 10 Tg(*Dyrk1a*), 14 Dp1Yah and 10 Dp1Yah/Tg(*Dyrk1a*) was used for the Morris water maze learning test (14–16 weeks). The behavioural protocols for open-field, Y-maze and NOR, rotarod, water maze were detailed in the Supplementary information.

Drug screening in yeast

All plasmids were generated using standard procedures. Restriction enzymes and Taq polymerase were obtained from New England Biolabs (Evry, France). T4 DNA ligase was purchased from Promega and purified synthetic oligonucleotides from Eurogentec. Routine plasmid maintenance was carried out in DH5α and TOP10 bacteria strains. Yeast cystathionine b-synthase (Cys4) coding sequence was amplified from the genomic DNA of the W303 *WT* strain (see genotype below) using Bam-Cys4-F: CGGGATCCCGATGACTAAATCTGAGCAGCAAG and Xho-Cys4-R: GCCTCGAGTCTTATGCTAAGTAGCTCAGTAAATCC (that introduced *Bam*HI and *Xho1* restriction sites) and subcloned in the high copy number 2 µ-derived vectors p424-GPD and p426-GPD, each time under the control of the strong constitutive *GDP* promoter (34). Transformation of yeast cells was performed using a standard lithium acetate method (35).

The yeast strain used in this study is derived from the W303 wt strain: *MATa*, *leu2-3,112 trp1-1 can1-100 ura3-1 ade2-1 his3-11,15*. The media used for yeast growth were the following: YPD [1% (w/v) yeast extract, 2% (w/v) peptone, 2% (w/v) glucose], for untransformed cells and synthetic dextrose *minimal medium* (SD medium) composed of 0.67% (w/v), *yeast* nitrogen base w/o amino acids and complemented with 0.1% (w/v) casamino acid, 40 mg/l adenine and 2% (v/v) glucose for Cys4-transformed cells. Solid media contained 2% (w/v) agar.

For the drug screening, yeast cells were grown in uracil- and tryptophan-free minimal liquid medium (SD-Ura/Trp) in overnight liquid cultures at 29°C. The following day, cells were diluted to OD_{600}~0.2 in fresh medium and grown for 4 h to reach exponential phase. Then 350 µl of exponentially growing yeast cells overexpressing Cys4, adjusted to an OD_{600} of 0.5, were spread homogeneously with sterile glass beads (a mix of ~1.5 and 3 mm diameter) on a square Petri dish (12 cm × 12 cm) containing uracil-, tryptophan- and methionine-free minimal agar-based solid medium (SD-Ura/Trp/Met) containing 2% (w/v) serine. Sterile filters (Thermo Fisher similar to those used for antibiograms) were placed on the agar surface, and 2 µl of an individual compound from the various chemical libraries were applied to each filter. In addition, for each Petri plate, DMSO, the vehicle, was added as a negative control on the top left filter, and 2 nmol of methionine as a positive control on the bottom right filter. Plates were then incubated at 33°C for 3 days and scanned using a Snap Scan1212 (Agfa).

Two repurposed drug libraries were screened: the Prestwick Chemical Library® (1200 drugs) and the BIOMOL's FDA approved drug library (Enzo Life Sciences, 640 drugs). In addition, the Prestwick Phytochemical library (691 green compounds, most of them being in use in human) was also screened. The compounds were supplied in 96-well plates as 10 mM (for the two Prestwick® libraries) and 2 mg/ml (BIOLMOL®) DMSO solutions. Disulfiram (DSF) was purchased from Sigma-Aldrich and resuspended in DMSO.

Mouse model treatment with disulfiram

A pre-clinical protocol was designed to target cognitive defects correlated to CBS overexpression in Tg(*CBS*) mice brain (Fig. 4D). The selected molecule was DSF, a potent inhibitor of mitochondrial aldehyde dehydrogenase (ALDH) used for the treatment of

chronic alcoholism. We based our experiment on the work of Kim *et al.* (36) in which the DSF effect on ethanol sensitization in mice was demonstrated.

Behavioural studies were conducted in 12–16 week-old animals; to do so, we generated three independent cohorts, in which we tested four conditions taking into account the dose of DSF (or vehicle alone) and the genotype. For the cohorts (C1–C3), we produced respectively 5,7,3 (n = 15 in total) wt mice treated with vehicle, 5,3,6 (n = 14 in total) transgenic mice for human *CBS* [Tg(*CBS*)] treated with vehicle, 7,5,3 (n = 15 in total) wt mice treated with 10 mg/kg/day of DSF, 6,6,8 (n = 20 in total) Tg(*CBS*) mice treated with 10 mg/kg/day of DSF based on the dose previously administrated in the reference publication (37). The local ethics committee, Com'Eth (n°17), approved the mouse experimental procedures, under the accreditation number APAFIS#1564-2015083114276031 with YH as the principal investigator in this study. All assessments were scored blind to genotype and animals were randomly distributed to experimental groups and treatment as recommended by the ARRIVE guidelines (37,38). DSF was prepared at 10 mg/mL in DMSO, aliquoted and stored below −20°C. The final formulation was prepared just prior to use as a 1 mg/mL solution diluted in Cremophor EL Castor oil (BASF)/H2O ready for injection (15/75), to reach a final DMSO/Cremophor/H2O 10/15/75 (v/v/v) mix. Treated animals received a daily dose (10 days) of this formulation by intraperitoneal injection of 10 mg/kg/day. Non-treated animals received the same formulation without DSF. On day 10 of treatment, the animals were habituated 30 min into the arena. On day 11, animals were tested in the NOR paradigm to assess recognition memory after 1 h retention as described in the open field and object recognition task protocols (Supplementary information).

Quantitative proteomic analysis

We collected five hippocampi of littermates of the four genotypes: wt, Dp1Yah, Tg(*Dyrk1a*)/0 and [Dp1Yah,Tg(Dyrk1a)/0] after their behavioural evaluation at the age of 25–27 weeks. Samples were reduced, alkylated and digested with LysC and trypsin at 37°C overnight. Five sets of samples with one sample from each genotype (four in total) were labelled with Thermo Scientific Tandem Mass isobaric tag (TMT), pooled and then analysed using an Ultimate 3000 nano-RSLC (Thermo Scientific, San Jose California) coupled in line with an Orbitrap ELITE (Thermo Scientific, San Jose California). An additional set was done comparing all the wt controls together. Briefly, peptides were separated on a C18 nano-column with a linear gradient of acetonitrile and analysed in a top 15 higher collision dissociation data-dependent mass spectrometry. Data were processed by database searching using SequestHT (Thermo Fisher Scientific) with Proteome Discoverer 1.4 software (Thermo Fisher Scientific) against a mouse Swissprot database. Precursor and fragment mass tolerance were set at 7 and 20 ppm, respectively. Trypsin was set as an enzyme and up to two missed cleavages were allowed. Oxidation (M) and TMT-labelled peptides in primary amino groups (+229.163 Da K and N-ter) were set as variable modification and carbamidomethylation (C) as a fixed modification. We then compared our five wt samples to determine the sample closer to average score from the group and defined it as the reference sample. All the protein quantification was performed based on the reference wt sample. In total, we detected 1655 proteins filtered with false discovery rate at 5% with a minimum of two peptides for a given protein detected per genotypes. We calculated the mean of the fold change for each protein from all the samples [Dp1Yah, Tg(*Dyrk1a*) and Dp1Yah/Tg(*Dyrk1a*)] compared to control. From the preliminary data, we selected 208 proteins with variability levels below 40% and a fold change below 0.8 or above 1.2.

Western blot analysis

Ten micrograms of total proteins from cortex extracts were electrophoretically separated in SDS-polyacrylamide gels (10%) and then transferred to nitrocellulose membrane (120 V) during 1 h 30 min. Non-specific binding sites were blocked with 5% skim milk powder in tween–tris-buffer saline (TTBS) 1 h at room temperature. Immunoblotting was carried out with primary antibody (Supplementary Material, Table S3) incubated overnight at 4°C. The next day, we started with three washing baths with TTBS, followed by secondary conjugated with horseradish peroxidase. The immunoreactions were visualized by ECL chemiluminescence system (Clarity™ western ECL substrate, Bio-Rad); epifluorescence was captured with Amersham™ Imager 600. Bands were detected at 18, 25 and 75 kDa, respectively for alpha-synuclein (SNCA), synaptosomal-associated protein 25 (SNAP25) and fused in sarcoma (FUS) and signals were quantified with ImageJ.

Results

Three copies of *Cbs* are necessary to induce cognitive impairments in the Dp1Yah mice

To challenge the hypothesis that three copies of *Cbs* are necessary to induce behavioural deficits in the Dp1Yah mice, we combined the Dp1Yah mice with the $Cbs^{tm1Unc/+}$ knock-out model (29) and we compared the Dp1Yah with Dp1Yah/Cbs^{tm1Unc} (in which only two copies of *Cbs* are functional), wt and $Cbs^{tm1Unc/+}$ heterozygote controls. In the open field test, all of the genotypes displayed similar exploratory behaviour, except for the Dp1Yah/*Cbs* mice that travelled more distance in the open field arena with a higher speed (Fig. 1A left panel; one-way ANOVA on distance, post hoc Tukey test: Dp1Yah versus Dp1Yah/$Cbs^{+/tm1Unc}$ $P = 0.002$; Fig. 1A right panel, one-way ANOVA on speed, post hoc Tukey test: wt versus Dp1Yah/$Cbs^{+/tm1Unc}$ $P = 0.004$, $Cbs^{+/tm1Unc}$ versus Dp1Yah/$Cbs^{+/tm1Unc}$ $P = 0.05$, Dp1Yah versus Dp1Yah/$Cbs^{+/tm1Unc}$ $P = 0.007$). We confirmed the increased activity of the Dp1Yah/Cbs^{tm1Unc} in the Y-maze revealed by a higher number of arm entries compared with the other genotypes (Fig. 1B, Kruskal–Wallis one-way ANOVA on ranks—genotypes, post hoc Dunn's method: wt versus Dp1Yah/$Cbs^{+/tm1Unc}$ $P < 0.05$, Dp1Yah versus Dp1Yah/$Cbs^{+/tm1Unc}$ $P < 0.05$) but no impact on spontaneous alternation (SA) [one-way ANOVA, $F(3, 87) = 2.486$ $P = 0.066$]. To determine if the motor activity was altered in the Dp1Yah/Cbs^{tm1Unc} model, we used the rotarod test. After the first day of training, we did not find any change, for all tested genotypes, in the maximum speed reached before falling [Fig. 1C, speed: repeated measures ANOVA variable «genotype» and «day», $F(3, 110) = 1.816$ $P = 0.155$]. Nevertheless, we observed a decrease in the locomotor learning of the Dp1Yah mice during the following days of training. This locomotor learning deficit was rescued in the Dp1Yah/Cbs^{tm1Unc} mutant [Fig. 1C, speed: repeated measures two-way ANOVA variable «genotype» and «day», $F(2, 165) = 17.171$ $P < 0.001$ post hoc Tukey method wt «day 1 versus day 3» $P = 0.002$, $Cbs^{tm1Unc/+}$ «day 1 versus day 3» $P < 0.001$, Dp1Yah «day 1 versus day 3»

P = 0.238, Dp1Yah/*Cbs*^{tm1Unc} «day 1 versus day 3» P = 0.017]. During the test phase, we found that the Dp1Yah individuals had a weaker performance compared with *Cbs*$^{tm1Unc/+}$ and Dp1Yah/*Cbs*^{tm1Unc} [ANOVA, variable «speed» and «genotype» $F(3, 385) = 5.544$ $P < 0.001$ post hoc Tukey method, «wt versus Dp1Yah» P = 0.099, «*Cbs*$^{tm1Unc/+}$ versus Dp1Yah» P = 0.001, «Dp1Yah versus Dp1Yah/*Cbs*^{tm1Unc}» P = 0.01].

Then we tested object memory. No difference was observed during the exploration of the familiar object in the presentation phase of the test (Fig. 1D, top left panel). However, during the discrimination phase, after 1 h of retention, the Dp1Yah mutant mice were not able to differentiate the novel object from the familiar one (Fo) whereas the wt, *Cbs*$^{tm1Unc/+}$ and the Dp1Yah/*Cbs*^{tm1Unc} spent significantly more time exploring the new object (No) than the Fo [Fig. 1D, left bottom panel; two ways ANOVA, variables 'genotype' and 'objects': $F(3, 56) = 2.86$ with P = 0.045; post hoc Tukey method wt 'fam versus new' q = 4.885 and P = 0.001; *Cbs*$^{tm1Unc/+}$ q = 3.913 and P = 0.008; Dp1Yah, q = 0.503 and P = 0.724; Dp1Yah/*Cbs*$^{tm1Unc/+}$ q = 4.715 and P = 0.002]. Accordingly, the recognition index showed that the restoration of two functional copies of *Cbs* in the Dp1Yah mice rescued memory performance in object recognition (Fig. 1D right panel, one sample t-test: wt P = 0.05, *Cbs*$^{tm1Unc/+}$ P = 0.01, Dp1Yah P = 0.82; Dp1Yah/*Cbs*$^{tm1Unc/+}$ P = 0.05).

Overall this set of experiments demonstrated that three copies of *Cbs* are necessary to induce the Dp1Yah phenotypes in the NOR test. In addition, rescuing *Cbs* dosage induced a slight hyperactive phenotype during the exploration of a new environment and restored performance in the rotarod activity. Interestingly, returning back to wt level of expression of *Cbs* in the *Abcg1-Cbs* region enables another trisomic gene from this region to impact on the locomotor activity during exploratory behaviour of the mouse.

The sole overexpression of a human CBS transgene impacts object recognition and locomotor activity

We used the Tg(*CBS*) model, a PAC transgenic line encompassing a 60 kb fragment with the human *CBS* locus (30), to analyse the impact of the sole increase of *Cbs* dosage on behaviour and cognition. As shown in Figure 2A, no difference in the locomotor activity was observed during the exploration of a new environment in the open field test between wt and transgenic littermates [Student t-test distance: wt versus Tg(*CBS*)/0 P = 0.925, speed wt versus Tg(*CBS*)/0 P = 0.925]. However, we found a higher circadian activity for isolated individuals [Fig. 2C, Student t-test wt versus Tg(*CBS*) $P < 0.001$] that results from an increased locomotor activity during the habituation and the dark phase (Fig. 2B). In the Y-maze (Figs 2D–E), no difference was detected between Tg(*CBS*)/0 and wt controls for the number of arm entries and the SA. In the NOR test, (Figs 2F–H) the Tg(*CBS*)/0 animals spent more time sniffing the two identical objects during the presentation phase than their control littermates [Fig. 2F, Student t-test wt versus Tg(*CBS*)/0 P = 0.05] but were impaired in object recognition as shown by their absence of discrimination between novel and familiar objects [Fig. 2G, Student-paired t-test wt 'Fo versus No' P = 0.008, Tg(*CBS*) 'Fo versus No' P = 0.174] resulting in a recognition index (time on the No/time on both objects) not significantly different from the 50% chance level, [Fig. 2H: one sample t-test, significant difference from 50%, wt P = 0.008, Tg(*CBS*)/0 P = 0.174]. Consequently, we demonstrated that CBS overexpression is sufficient to induce a deficit in the NOR memory and decreased locomotor activity during the dark phase while having no effect during the light phase.

Cbs overexpression in hippocampal and cortical neurons induces behavioural defects similar to Dp1Yah

We then checked if we could induce the cognitive deficits observed in DS mouse models by overexpressing *Cbs* in the hippocampal and cortical neurons, brain parts involved in learning and memory. Hence, we engineered the Tg(*Prp-gfp-CBS*) mouse strain in which the human CBS cDNA can be expressed from the prion promoter after the excision of the gfp cassette flanked by loxP sites (Fig. 3A) and selected one Tg(*Prp-gfp-CBS*) line with a pattern of expression in the anterior part of the adult brain (Fig. 3B). We chose the Tg(*Camk2a-cre*) (31), to direct the Cre expression in cortical and hippocampal glutamatergic neurons and we verified the expression of the human *CBS* in different brain regions of the double transgenic [Tg(*Prp-gfp-CBS*)/0, Tg(*Camk2a-cre*)/0]. As expected, we found expression levels comparable to the endogenous murine *Cbs* gene in cerebellum while human CBS was overexpressed in the hippocampus and the cortex (Fig. 3C). Littermate wt animals, carrying the two single transgenic constructs and the two transgenes were produced and tested for object recognition. During the test, the control groups, namely wt, Tg(*Prp-gfp-CBS*)/0 and Tg(*Camk2a-cre*)/0, spent more time on the No than the Fo as expected, while the double transgenic individuals were not able to differentiate the No from the Fo as shown by the recognition index or the percentage of exploration time {Fig. 3D; recognition index, one sample t-test: wt P = 0.03; Tg(*Camk2a-cre*)/0 P = 0.03; Tg(*Prp-gfp-CBS*)/0 P = 0.001; [Tg(*Prp-gfp-CBS*)/0; Tg(*Camk2a-cre*)/0] P = 0.90; exploration time; two ways ANOVA, variables 'genotype' and 'objects': $F(3, 76) = 8.59$ with $P < 0.001$; post hoc Tukey method wt «No versus Fo» $P < 0.001$; Tg(*Camk2a-cre*)/0 «No versus Fo» P = 0.001 and Tg(*Prp-gfp-CBS*)/0 «No versus Fo» $P < 0.001$; [Tg(*Prp-gfp-CBS*)/0; Tg(*Camk2a-cre*)/0] «No versus Fo» P = 0.861}.

Measurements of the travelled distance in the open field and number of visited arms in the Y-maze revealed hyperactivity of the Tg(*Camk2cre*)/0 carrier groups [Figs 3E–F, openfield: one-way ANOVA $F(3, 49) = 4.80$ P = 0.005, post hoc Holm–Sidak «wt versus Tg(*Camk2-Cre*)/0» unadjusted P = 0.002, «Tg(*Prp-gfp-CBS*)/0 versus Tg(*Camk2-Cre*)/0» P = 0.003); Y-maze: one-way ANOVA $F(3, 46) = 6.04$ P = 0.001, post hoc Holm–Sidak «wt versus Tg(*Camk2-Cre*)/0» P = 0.04, «Tg(*Prp-gfp-CBS*)/0 versus Tg(*Camk2-Cre*)/0» P = 0.009, Tg(*Prp-gfp-CBS*)/0 versus Tg(*Prp-gfp-CBS*)/0, Tg(*Camk2a-cre*)/0 P = 0.04). Similarly to the Dp1Yah and Tg(*CBS*) animals, we did not find any alteration in the SA in the Y-maze test [one-way ANOVA: $F(3, 43) = 0.691$ P = 0.563]. All the mice, whatever their genotype, performed equally well during the training session of the rotarod (Fig. 3G) [training: repeated measures ANOVA, variables «genotype» and «day», $F(3, 90) = 2.011$ P = 0.126; test: repeated measures ANOVA, variables «genotype» and «day», $F(2, 90) = 44.783$ $P < 0.001$] as well as during the test session with increasing speed [repeated measures ANOVA, variables «genotype» and «speed», $F(18;322) = 0.631$ P = 0.875]. Thus, as expected from the role of the cerebellum in locomotor coordination, the overdose of CBS restricted to cortical and hippocampal neurons did not interfere with the locomotor activity.

Hence, overexpression of CBS is necessary and sufficient to induce object memory defect in a 1 h retention test with limited impact on other phenotypes. As such, *CBS* is a new gene that overdosage alters cognition in DS mouse models and as a consequence is likely to contribute to DS phenotypes.

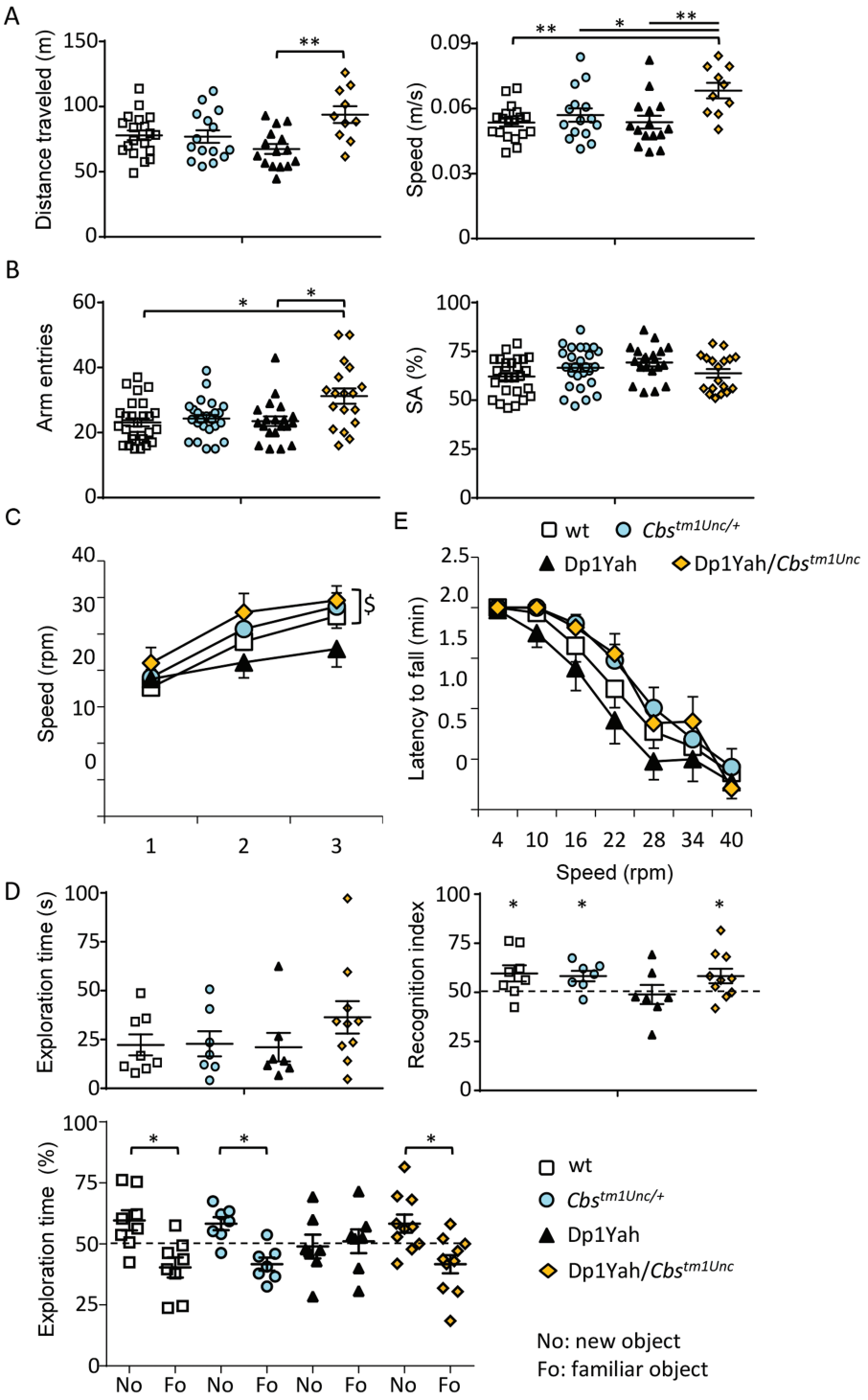

Figure 1. The Dp1Yah phenotypes are dependent on *Cbs* dosage. Dp1Yah trisomic mice ($n = 23$) were compared with Dp1Yah carrying a KO of *Cbs* (Dp1Yah/Cbs^{tm1Unc}, $n = 21$), $Cbs^{tm1Unc/+}$($n = 23$) and wt littermates ($n = 29$). Animals were analysed in two independent cohorts in the following tests: open field (**A**), Y-maze (**B**) and NOR (**D**). The rotarod (**C**) test was assessed on one cohort with wt ($n = 18$) $Cbs^{tm1Unc/+}$ ($n = 15$), Dp1Yah ($n = 15$) and Dp1Yah/Cbs^{tm1Unc} ($n = 10$) littermates. (A) Distance travelled and medium speed during the 30 min of the test were increased in the *Dp1Yah/*Cbs^{tm1Unc} compared with the wt genotype. (B) Increased exploration activity was confirmed for the *Dp1Yah/*Cbs^{tm1Unc} mice compared with control littermates in the Y-maze while SA was not affected. (C) During the training session (left panel), the Dp1Yah mice were not able to improve their performance on the rotarod by increasing the maximum of speed before they fall from the rod compared to the other genotypes. Nevertheless, no change was observed between individuals with the four genotypes during the test phase (right panel). (D) The exploration time in the first session of the NOR test (left upper panel) was not statistically different in the four genotypes but during the recognition phase, after 10 min of retention, the recognition index (right upper panel, time spent on the No/total time of exploration) was clearly lower in Dp1Yah mice as compared with the other genotypes and not statistically different from chance (50%). Accordingly, the exploration time (left lower panel) spent by the *Dp1Yah/*Cbs^{tm1Unc} mice to explore the object showed that they were able to differentiate the novel (No) versus familiar (Fo) object while the Dp1Yah were not. Data are represented as one point per individual tested and the mean of the group. (Values represent means + S.E.M. $^{*}P < 0.05$, $^{**}P < 0.01$, $^{***}P < 0.001$).

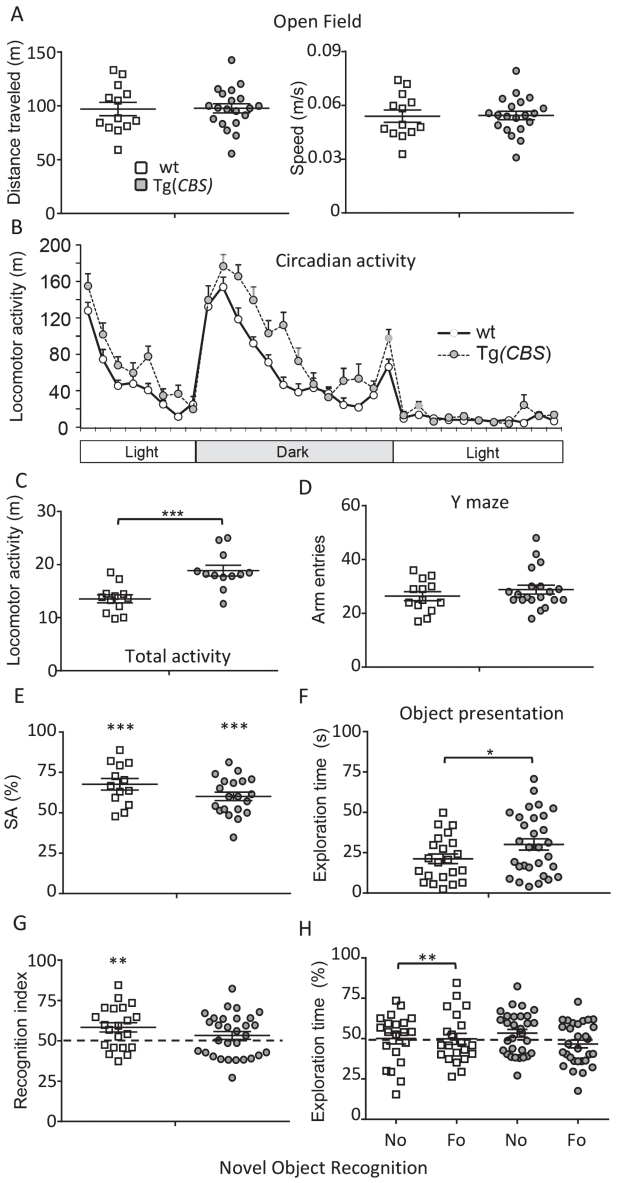

Figure 2. Transgenic mice overexpressing human CBS display DS-related behaviour phenotypes. Wt ($n = 13$) and Tg(CBS)/0 littermates ($n = 17$), hemizygotes for a human PAC containing the *CBS* gene, were tested for the open field (**A**), circadian actimetry (**B–C**), Y-maze (**D–E**) and NOR (**F**, **G** and **H**). No phenotype was found in the Tg during the exploration of a new environment in the open field looking at the total distance travelled (left) and the speed (right). However, increased activity was observed during home cage monitoring over a light–dark–light cycle (B) with an increase in the distance travelled (C). In the Y-maze (E), Tg(CBS)/0 animals displayed altered SA with no change in the number of arm entries (D). In the NOR test (F), Tg(CBS)/0 mice displayed similar exploration activity compared to wt littermates but they did not discriminate the novel versus the familiar object when looking at the discrimination index (G) and the percentage of exploration time for both objects (H). (Values represent means + S.E.M. $^*P < 0.05$, $^{**}P < 0.01$, $^{***}P < 0.001$).

Identification of drugs that suppress the effects of Cys4/CBS overexpression both in yeast and mouse

A few studies have reported the identification of CBS inhibitors (39–44) but most of them were based on *in vitro* assays using a recombinant CBS enzyme as a drug target and led to the isolation of inhibitors with relatively low potency and limited selectivity, hence leading to the idea that CBS may be an undruggable enzyme. Therefore, we oriented toward an *in cellulo* phenotype-based assay that would allow the identification of drugs that interfere with the phenotypical consequences of CBS overexpression and thereby that do not necessarily directly target the CBS enzyme. The budding yeast *Saccharomyces cerevisiae* contains a functional homolog of CBS and has been shown to be a relevant system to model pathophysiological mechanisms involved in a number of human disorders and to perform chemobiological approaches that aim at identifying both drugs and new therapeutic targets (45–51). We thus decided to create a yeast model in which the phenotypical consequences of CBS overexpression may be easily and conveniently monitored in order to get potential *in cellulo* high throughput drug screening procedure. We reasoned that if we overexpressed CBS at a sufficient level, this should lead to a decreased intracellular level of methionine, similarly to what was shown in patients, and therefore that yeast cells would become methionine auxotroph and thereby unable to grow on methionine-free minimal media. As the human CBS protein is not very stable in yeast cells and therefore cannot be expressed at high levels (52), we decided to overexpress Cys4p, the CBS homolog in *S. cerevisiae*. Cys4p presents the same domains and domain organization as CBS apart from the N-terminal heme-binding domain that is absent in the yeast protein (53). To get a degree of methionine auxotrophy sufficient to allow an efficient screening, we expressed Cys4 from the strong constitutive *GPD* promoter from two different high copy number 2 μ vectors (each present at ∼50 copies per cell) and supplemented the growth medium with serine, which is one of the Cys4p/CBS substrates that could otherwise become limiting upon Cys4 overexpression (Fig. 4A).

Using this model, we tested ≈ 2200 compounds from three different chemical libraries consisting mainly of repurposed drugs for their ability to suppress the methionine auxotrophy induced by Cys4p overexpression. We exploited a similar principle as a yeast-based screening setup previously (46,47,49,54). Briefly, we spread yeast cells overexpressing Cys4 on a solid agar-based methionine-free minimal medium. Then we put filters on the agar surface and add different drugs from chemical libraries on each filter. After 3 days of incubation at 33°C, active compounds were identified by a halo of restored/enhanced growth around the filter on which they were loaded (Fig. 4B). The advantage of this method is that it allows in one simple experiment numerous compounds to be tested across a large range of concentrations due to the diffusion of the molecule in the medium surrounding the filter onto which it was deposited. This design drastically improves the sensitivity of the screen because the screened compounds can be toxic at high concentrations whereas being active at subtoxic concentrations. We identified four different compounds, among which DSF (Fig. 4C).

Next, we tested if DSF was able to restore the object recognition in the mouse model overexpressing human *CBS*. Three independent cohorts of Tg(*CBS*) and control littermates were treated with DSF (10 mg/kg/day) for 10 days before being tested for the NOR. As shown in Figure 4D, DSF-treated transgenic animals were restored in the NOR paradigm whereas non-treated mutant animals were still not able to discriminate the No versus the Fo. Interestingly, the wt-treated individuals were no more able to perform the discrimination while the vehicle-treated controls were able to do so [Student-paired *t*-test: vehicle-treated wt «No versus Fo» $P = 0.006$, DSF-treated wt «No versus Fo» $P = 0.11$ and vehicle-treated Tg(CBS) «No versus Fo» $P = 0.59$, DSF-treated Tg(*CBS*) «No versus Fo» $P = 0.05$]. Altogether, these results confirm

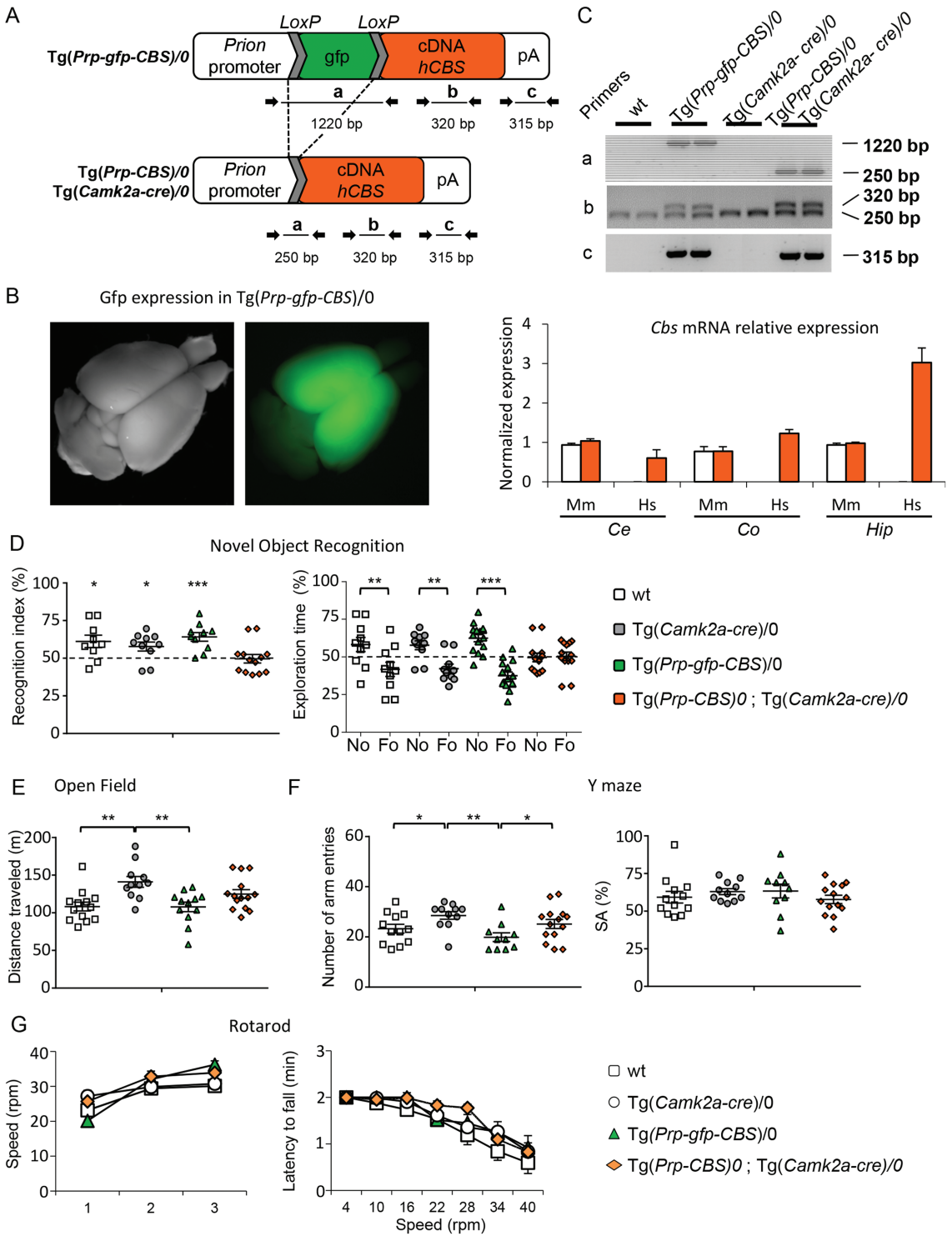

Figure 3. Selective overexpression of *h*CBS in glutamatergic neurons leads to impaired object recognition and altered locomotor activity. (**A**) A conditional transgene Tg(*Prp-gfp*-CBS) was designed to overexpress the human CBS cDNA from the murine Prion promoter after the deletion of an interrupting GFP-coding cassette flanked by loxP sites. (**B**) The GFP allowed to select one line that leads to expression in the anterior part of the brain. (**C**) When Cre is expressed from the Tg(Camk2-Cre) transgene, the deletion can be monitored in regions of the brain of the animals (upper panel) using different pairs of primers while the overexpression of hCBS mRNA (labelled Hs) is detected by qRT-PCR in different parts of the brain (Ce: Cerebellum, Co: Cortex, Hip: Hippocampus; lower panel) in the Tg(Camk2-Cre)/0, Tg(*Prp-gfp*-CBS)/0 animals (orange bar). No change in the endogenous murine CBS (Mm) is detected in Tg(Camk2-Cre)/0, Tg(*Prp-gfp*-CBS)/0 animals (orange bar) compared to wt animals (white bar). (**D**) wt (n = 13), Tg(Camk2-Cre)/0 (n = 11), Tg(*Prp-gfp*-CBS)/0 (n = 12) and Tg(Camk2-Cre)/0, Tg(*Prp-gfp*-CBS)/0 (n = 14) littermates were evaluated for object discrimination (D), in the open field (**E**), Y-maze (**F**) and rotarod (**G**). Mice overexpressing hCBS in glutamatergic neurons were unable to discriminate the novel versus the familiar object as compared with the other control genotypes (D). Tg(Camk2-Cre)/0 mice displayed an enhanced locomotor activity in the open field but no change was detected in the control, wt and Tg(*Prp-gfp*-CBS)/0, or in double transgenic animals (E). In the Y-maze, animals carrying the Tg(*Prp-gfp*-CBS)/0 or the activated form, Tg(Camk2-Cre)/0, Tg(*Prp-gfp*-CBS)/0, displayed reduced exploration with a lower number of arm entries but no change in the SA (F). No alteration was detected in the rotarod test with similar progress during the learning and the test phases (G). (Values represent means + S.E.M. $^{*}P < 0.05$, $^{**}P < 0.01$, $^{***}P < 0.001$).

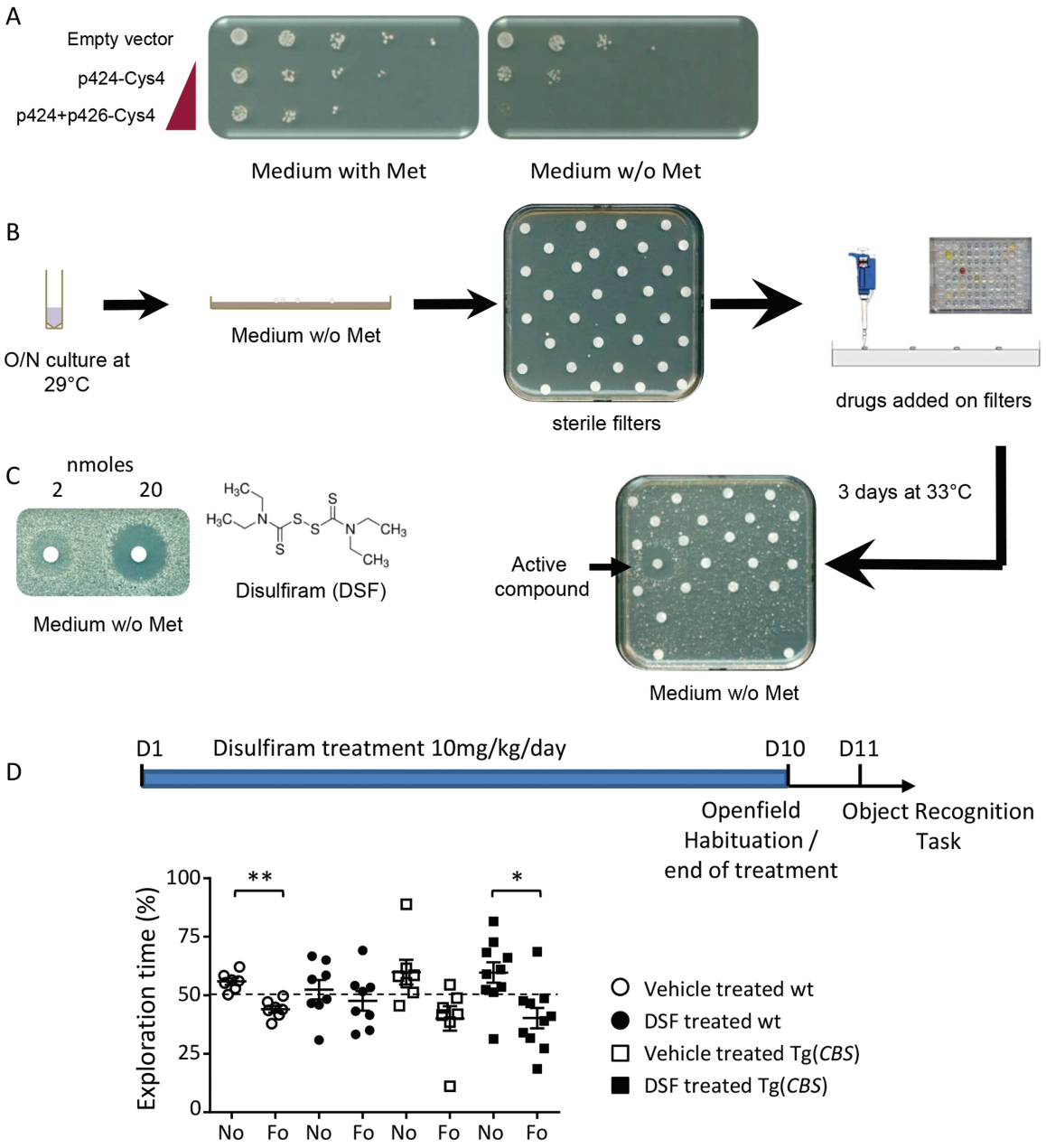

Figure 4. Pharmacological intervention to suppress the consequences of CBS overexpression in yeast (**A–C**) and mouse (**D**). Development of a yeast screening assay based on Cys4-overexpressing cells and identification of DSF as able to suppress methionine auxotrophy induced by Cys4 overexpression. The sensitivity of the strain to the absence of methionine in the medium was evidenced by serial dilutions of a yeast strain expressing different levels of Cys4 (A). For the drug screening, the yeast strain overexpressing Cys4 from both p424 & p426 2 µ multicopy plasmids was spread on a square Petri plate containing solid agar-based methionine-free medium. DMSO was used as a negative control and added to the upper right filter and methionine, the positive control, was loaded on the bottom left filter (B). At the remaining positions, individual compounds from the chemical libraries were added and plates were incubated for 3 days at 33°C. Three types of growth profiles can be observed around the filters where the compounds were loaded. Either the compounds have no effect, which results in the same basal growth (indeed, the overexpression of Cys4 does not lead to a complete methionine auxotrophy as evidenced in C), or it is toxic, which results in a total absence of growth (visualized as a dark halo corresponding to the colour of the solid media). The last possibility corresponds to active drugs that suppress the methionine auxotrophy, thereby leading to a halo of enhanced growth around the filter. Of note, a single compound can display various effects (which is the case for DSF, see below), it can be toxic at high concentration (immediately around the filter), thereby leading to a halo of non-growing cells at the immediate vicinity of the filter and then become active at sub-toxic concentrations that leads to a crown of cells growing at a faster rate (leading to the formation of bigger colonies) and then become inactive at sub-active concentrations (at a bigger distance from the filter). The dose-dependent effect of DSF on Cys4-overexpressing cells is shown, and its molecular structure is depicted (C). To test DSF in mice, treatment was done on Tg(*CBS*) cohort starting at D1 and ending at D10 (D). Each group received a daily dose of 10 mg/kg/day of DSF for 10 days followed by an open field paradigm (D10) with the object recognition test performed on D11 (with 1 h of retention time). The graph at the bottom showed the percentage of time spent on the novel versus the familiar object during the tests. The vehicule-treated wt mice were able to discriminate both objects as the DSF-treated Tg(*CBS*) animals. On the contrary, non-treated transgenic animals were not able to do so and the DSF-treated wt animals were impaired in the test confirming that the drug affects the consequences of CBS activity *in vivo* (values represent means + S.E.M. $^{*}P < 0.05$, $^{**}P < 0.01$, $^{***}P < 0.001$).

that the phenotypical consequences of the overexpression of CBS could be targeted by drugs to restore some of the cognitive performance altered in DS models. They also emphasize that the inhibition of CBS, direct or indirect, should be mild and only partial as a strong inhibition may be detrimental as illustrated by the cognitive dysfunction observed in homocystinuria.

Epistatic interaction between *Dyrk1a* and the *Abcg1-Cbs* region drives recognition memory in DS mouse models

Dyrk1a is a major driver gene of DS cognitive defects (55) and a decrease in *Cbs* dosage is known to change the expression of *Dyrk1a* in the brain and other organs (56–58). Thus in order to test the functional interaction of *Cbs* and *Dyrk1a* overdosage, we combined the Dp1Yah with the Tg(*Dyrk1a*) mouse model, with *Dyrk1a* mRNA expression ratio around 1.5 compared with control littermate (32) and the overexpression of the protein and its kinase activity (33). Tg(*Dyrk1a*) mice present increased spontaneous activity compared with wt in the open field test. This hyperactivity was also observed in the double transgenic Dp1Yah/Tg(*Dyrk1a*) while it was absent from Dp1Yah animals [Fig. 5A, Student *t*-test wt versus Dp1Yah $P = 0.460$, wt versus Tg(*Dyrk1a*) $P = 0.002$ and wt versus Dp1Yah/Tg(*Dyrk1a*) $P = 0.006$, Tg(*Dyrk1a*) versus Dp1Yah/Tg(*Dyrk1a*) $P = 0.200$]. Hyperactivity was confirmed in the Y-maze, with both Tg(*Dyrk1a*) and Dp1Yah/Tg(*Dyrk1a*) performing more arms visits than the controls and Dp1Yah mice [Fig. 5B, Student *t*-test wt versus Dp1Yah $P = 0.800$, wt versus Tg(*Dyrk1a*) $P = 0.005$ and wt versus Dp1Yah/Tg(*Dyrk1a*) $P = 0.005$, Tg(*Dyrk1a*) versus Dp1Yah/Tg(*Dyrk1a*) $P = 0.881$]. The working memory defect observed in the Y-maze for Tg(*Dyrk1a*) mice was not rescued in Dp1Yah/Tg(*Dyrk1a*) double transgenic mice [Fig. 5B, one-way ANOVA $F(3, 48) = 4.14$ $P = 0.011$, post hoc Tukey method wt versus Tg(*Dyrk1a*) $P = 0.042$, wt versus Dp1Yah/Tg(*Dyrk1a*) $P = 0.019$ and Tg(*Dyrk1a*) versus Dp1Yah/Tg(*Dyrk1a*) $P = 0.203$]. Then, we tested the NOR memory after 1 h of retention (Fig. 5C). As expected, the two single mutants were impaired [two ways ANOVA, variables 'genotype' and 'objects': $F(3, 70) = 7.09$ with $P < 0.001$, post hoc Tukey test: Dp1Yah 'fam versus new' $q = 1.333$ and $P = 0.349$, Tg(*Dyr1a*) $q = 1.732$ and $P = 0.225$; recognition index, one sample *t*-test mean versus 50%: Dp1Yah $P = 0.253$, Tg(*Dyrk1a*) $P = 497$] but the double transgenic mice Dp1Yah/Tg(*Dyrk1a*) were able, similarly to wt littermates, to discriminate the familiar versus novel objects [two ways ANOVA, variables 'genotype' and 'objects': $F(3, 70) = 7.09$ with $P < 0.001$, post hoc Tukey test: wt 'fam versus new' $q = 4.543$ and $P = 0.002$, Dp1Yah/Tg(*Dyr1a*) $q = 5.289$ and $P < 0.001$; recognition index, one sample *t*-test: wt $P = 0.048$, Dp1Yah/Tg(*Dyrk1a*) $P = 0.011$], suggesting that the effects of *Dyrk1a* overexpression are compensated by three copies of the *Abcg1-Cbs* region.

Lastly, we checked the learning and spatial memories using the Morris water maze task, followed by a probe test 24 h after the learning period (Fig. 5D). Even if all the groups increased their performance to reach the platform during the learning phase, after 6 days of training (J1–J6), wt and Dp1Yah mice found the platform with lower latency than the Tg(*Dyrk1a*) and Dp1Yah/Tg(*Dyrk1a*) [two ways ANOVA variable genotype, $F(3, 280) = 14.80$ $P < 0.001$, post hoc Tukey test: wt versus Tg(*Dyrk1a*) $q = 6.160$ with $P < 0.001$, wt versus Dp1Yah/Tg(*Dyrk1a*) $q = 4.752$ with $P = 0.004$, Dp1Yah versus Tg(*Dyrk1a*) $q = 8.103$ with $P < 0.001$, Dp1Yah versus Dp1Yah/Tg(*Dyrk1a*) $q = 6.641$ with $P < 0.001$]. During the probe test, 24 h after the learning phase, controls and Dp1Yah animals were most of their time, searching in the platform quadrant (T), whereas Tg(*Dyrk1a*) and double transgenic mice searched randomly across the entire space [one sample *t*-test versus 50% mean: wt $P = 0.02$, Dp1Yah $P = 0.05$, Tg(*Dyrk1a*) $P = 0.99$ and Dp1Yah/Tg(*Dyrk1a*) $P = 0.57$]. Hence, overexpressing Cbs and Dyrk1a does not rescue the Dyrk1a dosage-dependent working and spatial memory deficits observed in the Y-maze and the Morris water maze, respectively, neither the hyperactivity observed in the open field, but rescued the object recognition impairment.

Proteomics unravels complex intermingled proteomic changes influenced by DYRK1A overexpression and by Dp1Yah trisomic genes

In order to unravel the impact of CBS and DYRK1A on cellular mechanism within the hippocampus that could lead to the memory phenotype observed in the NOR test, we profiled the proteome in the hippocampi isolated from Dp1Yah, Tg(*Dyrk1a*) and double [Dp1Yah, Tg(*Dyrk1a*)] animals and compared them with the wt control littermates. We collected the samples after the behavioural evaluation and performed a TMT labelling (Thermo Scientific, Illkirch) followed by LC-MS/MS orbitrap analysis. We were able to detect 1655 proteins of which 546 were detected in all the three genotypes with a variability below 40% (Supplementary Material, Table S4) and among which 338 proteins were expressed at the same level as control ones. A total of 208 proteins were found differentially expressed with levels of expression above 1.2 (206) or below 0.8 (2) in Dp1Yah, Tg(*Dyrk1a*) and double mutant mice (Fig. 6A). Nine proteins were up-regulated in all three genotypes: the RIKEN cDNA 6430548 M08 gene product (6430548M08RIK), actin-related protein 2/3 complex, subunit 1A (ARPC1A), bridging Integrator 1 (BIN1), the family with sequence similarity 213, member A (Fam213a), glyoxalase 1 (GLO1), importin 5 (LPO5), NADH dehydrogenase (ubiquinone) Fe-S protein 1 (NDUFS1), prostaglandin reductase 2 (PTGR2) and SNAP25. ToppCluster analysis of the protein content unraveled a general common network with interacting proteins modified by the three genetic conditions (Fig. 6B–C). Functional analysis using gene ontology highlighted several cellular components affected in the three genotypes including synaptic particles, neuron projection, presynapse/synapse, axon, myelin sheath and different types of vesicles (Supplementary Material, Table S5). Cell/neuron projection development, morphogenesis and differentiation, as well as secretion, synaptic and anterograde trans-synaptic signalling were affected in Dp1Yah while aldehyde catabolic processes and regulation of anatomical structure size were modified in Tg(*Dyrk1a*). Interestingly, all these biological processes were not disturbed in double transgenic animals. Likewise, molecular functions controlling ubiquitin protein ligase, calcium ion binding and dicarboxylic acid transmembrane transporter activity deregulated in Dp1Yah or cytoskeletal protein and myosin binding perturbed in Tg(*Dyrk1a*) were restored [Dp1Yah, Tg(*Dyrk1a*)]. On the contrary, oxidoreductase activity was newly modified in the double transgenic hippocampi.

We selected three proteins with different proteomic profiles in hippocampi and studied their expression in another brain region, the cerebral cortex, using western blot analysis: the SNCA and the FUS proteins, which are associated with neurodegenerative disease (59–62) and the SNAP25, a component of the SNARE complex involved in calcium-triggered exocytosis (63–65). As shown in Figure 5D, levels of SNCA were similar to wt level. We did observe the increased amount of this protein in

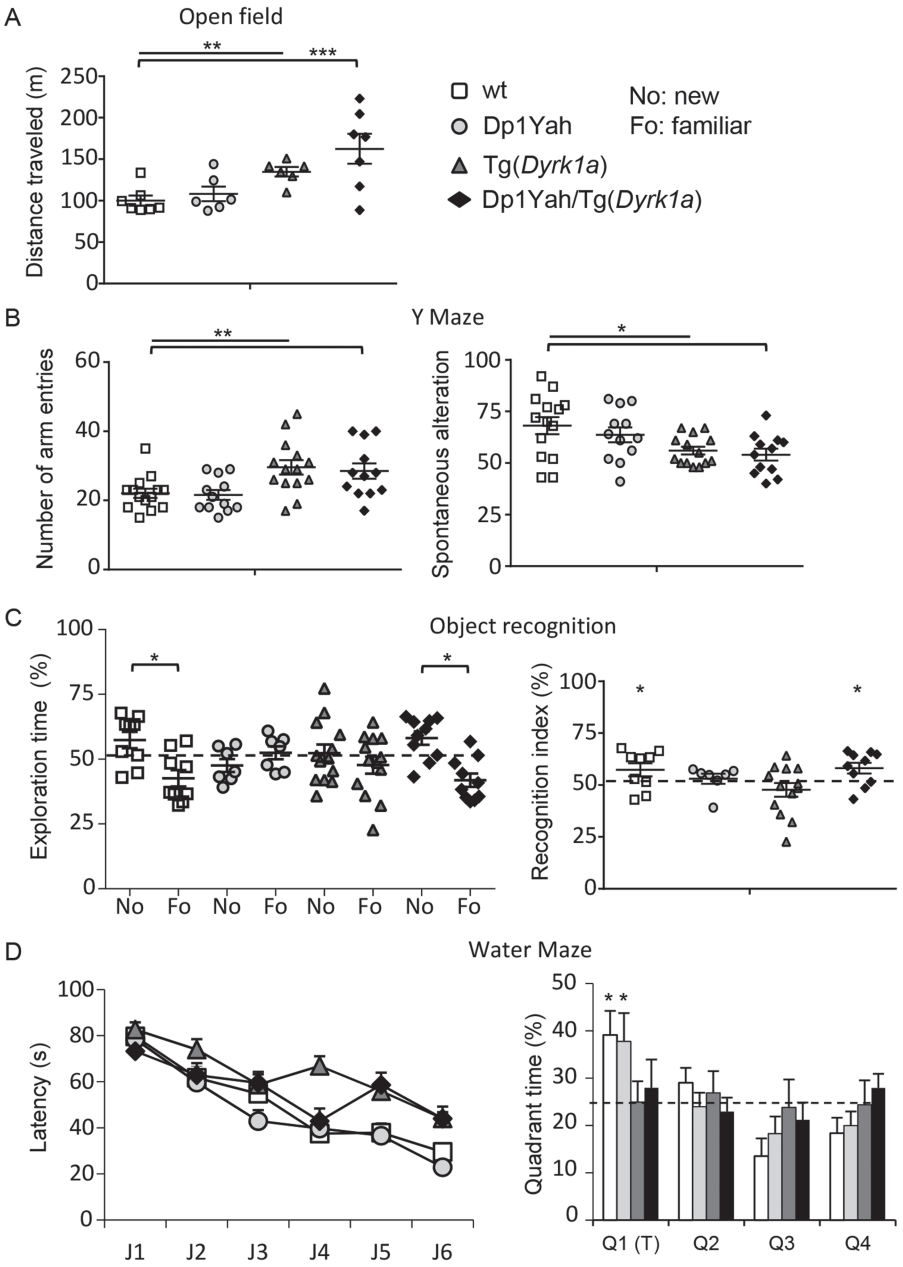

Figure 5. CBS and DYRK1A overdosages interact to control behaviour and cognition. Behavioural and cognitive analysis of transgenic animals overexpressing *Cbs* and *Dyrk1a* (14 wt, 15 Tg(*Dyrk1a*), 13 Dp1Yah and 13 (Dp1Yah,Tg(*Dyrk1a*)) mutant mice in the open field (**A**), the Y-maze (**B**), the object recognition (**C**) and the Morris water maze (**D**). Increased activity in the open field (A) and in the number of arm entries in the Y-maze (B) were found in the Tg(*Dyrk1a*) and (Dp1Yah,Tg(*Dyrk1a*)) animals with also reduced SA in the Y-maze (B). Both the Dp1Yah and (Dp1Yah,Tg(*Dyrk1a*)) mutant mice were impaired in object recognition (C) but the double mutant animals showed restored object discrimination similar to wt littermates. The Tg(*Dyrk1a*) and (Dp1Yah,Tg(*Dyrk1a*)) animals displayed delayed learning in the Morris water maze with no memory of the platform location in the probe test compared with Dp1Yah and wt littermates (D). (Values represent means + S.E.M. $^{*}P < 0.05$, $^{**}P < 0.01$, $^{***}P < 0.001$).

the [Dp1Yah, Tg(*Dyrk1a*)] animals contrary to what was observed in the proteome analysis. The presynaptic SNAP25 protein was significantly up-regulated in cortical regions of the [Dp1Yah, Tg(*Dyrk1a*)] animals and to a lesser extent in the Dp1Yah and Tg(*Dyrk1a*) ones {Student *t*-test wt versus Tg(*Dyrk1a*) $P = 0.233$, wt versus Dp1Yah $P = 0{,}06$, wt versus [D1Yah, Tg(Dyrk1a)] $P = 0.02$}. Hence, in the proteomic approach, we also observed the increase previously detected in the hippocampus of those three transgenic lines. The RNA-binding protein FUS was found overexpressed in the Dp1Yah brains and to a lesser extent in the [Dp1Yah, Tg(*Dyrk1a*)] ones, similarly to what was observed in the proteomic analysis {Student *t*-test Dp1Yah compared to wt $P = 0.02$ and [Dp1Yah, Tg(Dyrk1a)] compared with wt $P = 0.09$}.

Discussion

In this report, we demonstrated that the genetic overdosage of *Cbs* is necessary and sufficient to induce defective NOR in three different types of DS models. CBS overdosage is certainly the main driver of the learning and memory phenotypes detected previously in DS models for the Mmu17 region (21,22) but we

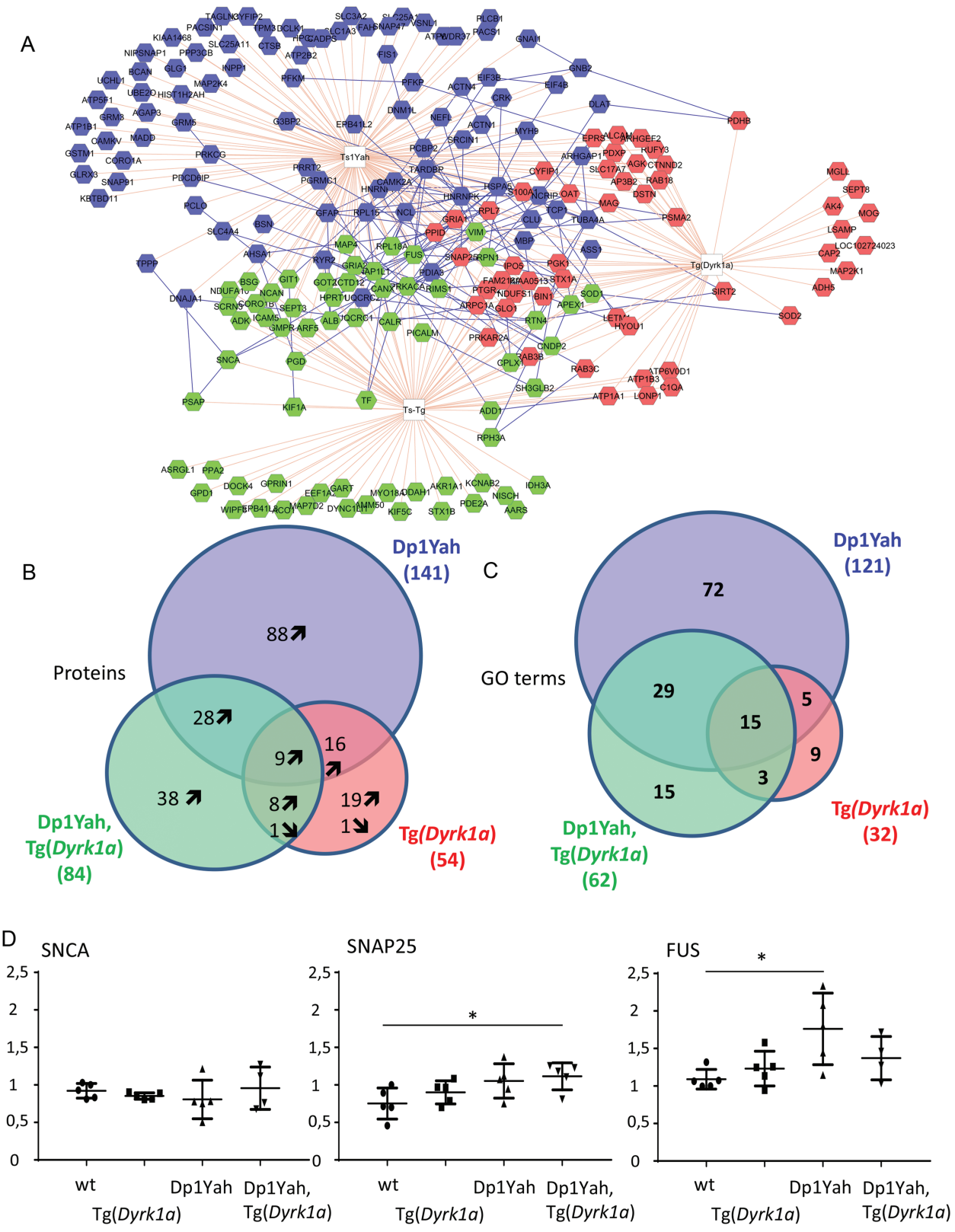

Figure 6. Pattern of protein expression is disrupted upon changes in DYRK1A and CBS dosage. (**A**) Analyzing the 1655 proteins detected in the Orbitrap ELITE experiment, we extracted from Proteome Discoverer 1.4© a list of 208 proteins dysregulated in our different sample conditions. The association between proteins, pathways and genotypes is summarized in two Venn diagrams (**B–C**). We deduced that the trisomic alleles induced most of the perturbations; moreover, the combination of increased DYRK1A and trisomic condition led to new dysregulations. (**D**) Western blot validation of three protein candidates SNCA, SNAP25 and FUS. SNAP25 expression is increased in samples overexpressing DYRK1A. More interestingly, FUS was found significantly up-regulated in Dp1Yah, plots represent every sample values normalized with β-actin level. (Values represent means + S.E.M. *$P < 0.05$, **$P < 0.01$, ***$P < 0.001$).

cannot rule out the possibility that one or more another gene(s) contribute, with *Cbs*, to the phenotype. Previous analysis of CBS overdosage with the same transgenic line Tg(*CBS*) on the FVB/N genetic background showed no change in fear-learning task and locomotor activity but increased LTP-dependent synaptic plasticity (66); a phenomenon also detected *in vitro* and *in vivo* in other DS models in which *Cbs* is trisomic in the C57BL/6J genetic background (21,22). Nevertheless, no positive effect on cognition is associated with increase in CBS dosage as previously proposed by Régnier *et al.* (66). Instead, the overdosage of CBS always impairs the hippocampal-dependent NOR test suggesting that increased synaptic plasticity found in *Cbs* trisomic models may alter synaptic functions. Increased synaptic plasticity could occur via increased H_2S as it has been shown that H_2S facilitates LTP by stimulating the post-synaptic NMDA receptors (67,68). Moreover, a role of H_2S has been foreseen in calcium homeostasis regulation that is also crucial for neuronal synaptic plasticity (69).

DSF was isolated from a drug screening performed in yeast cells overexpressing CBS homolog Cys4p and looking for drugs counteracting its effect on methionine auxotrophy. Although DSF has been first identified as an inhibitor of mitochondrial ALDH (70), it is a relatively nontoxic substance, which has been on the market for more than 40 years to support the treatment of chronic alcoholism by producing an acute sensitivity to ethanol, leading to an accumulation of acetaldehyde in blood when alcohol is ingested. As acetaldehyde is responsible for many of the unpleasant effects that follow ingestion of large quantities of alcohol ('hangover'), DSF treatment discourages the patients to sustain a regular alcohol consumption by exacerbating and accelerating its unpleasant side effects. DSF is known to have a sedative effect both in mouse and patients. It is thus possible that this side effect reduces the ability of treated wt mice to perform the object recognition test as efficiently as non-treated mice. Further studies are necessary to better understand the mode of action and identify the targets of DSF affected in this behavioural test. Our ongoing studies about the mechanism of action of DSF suggest that this molecule may not directly inhibit CBS enzymatic activity but probably rather acts on the cellular consequences of CBS overexpression. The assay used for the screening allows, in principle, the isolation of drugs acting both directly or not on CBS/Cys4. This latter point is of importance given that CBS may not be a druggable target enzyme. And indeed, at present, we do not know if DSF is acting directly or indirectly on CBS but we must assume that the function altered by CBS overdosage, whatever it is, is conserved and similarly sensitive to DSF treatment in both yeast and mouse. Of note, upon absorption, DSF is rapidly reduced to diethyldithiocarbamate (DDC), which then reacts with thiol groups. Both DSF and DDC are potent copper chelators, thereby possibly affecting the activity of copper-dependent enzymes such as monooxygenases, the Cu–Zn superoxide dismutase, amine oxidase, ADN methyltransferases, and cytochrome oxidase. As a result, DSF has been shown to affect various cellular processes such as cocaine metabolism and catecholamine synthesis and proteasome inhibition and is thus under study for multiple clinical applications that include struggle against alcohol addiction, cancer chemotherapy, treatment of copper-related disorders and anti-viral treatment for hepatitis C and human immunodeficiency virus (71). Here, we describe a new possible clinical application of DSF in DS cognition through its effect on the consequences of CBS overexpression. CBS clearly represents a new relevant therapeutic target for improving DS cognition and DSF, as such, opens new therapeutic avenues in patients with DS.

We also demonstrated that *CBS* genetically interacts with *Dyrk1a*, a well-known therapeutic target for DS. Mutual relationships between DYRK1A and CBS have previously been reported, with decreased DYRK1A protein observed in the liver (Hamelet *et al.*, 2009) and increased expression observed in the brain of $Cbs^{+/-}$ mice (Planque *et al.*, 2013), while overexpression (or under-expression) of DYRK1A induce accumulation (or reduction) of CBS expression in the liver (72). In order to explore the genetic interactions between DYRK1A and CBS, we overexpressed *Dyrk1a* in the Dp1Yah context by combining the Tg(*Dyrk1a*) and the Dp1Yah mice. Surprisingly, this experiment restored memory that is lacking in the Dp1Yah mouse model in the object recognition task, but neither normalized the increased locomotor activity in the open field or the Y-maze nor the working and spatial memory deficits. Thus, the compensation is restricted to a specific cognitive function, recognition memory, which is defective in both TgDyrk1a and Dp1Yah models. Why this dosage effect is restricted to recognition memory remains speculative. We may hypothesize that *Cbs* and *Dyrk1a* overdosage only interact in specific regions of the adult brain involved in object discrimination explaining why the increased locomotor activity and the working and visuo-spatial phenotypes induced in Tg(*Dyrk1a*) animals are not affected. Alternatively, the object recognition deficit is likely to result from an impact of DYRK1A on adult brain function while the other phenotypes are the result of an impact during earlier stages of brain development. On the one hand, object recognition has been shown to require undamaged hippocampal perforant path connecting ento/perirhinal cortex with the dentate gyrus for long retention intervals (>15 min) in the rat (73–78). On the other hand, synaptic exchanges between the median prefrontal cortex and the hippocampus seem to be sufficient to support the processing of short-term memory such as working memory observed in the Y-maze (79,80) and hyperactivity is associated with the prefrontal cortex, basal ganglia and cerebellum (81–84). Moreover, long-term recognition memory has been shown to appear in the rat at weaning (post-natal day 21 in the mouse) (85), a period corresponding to the end of neurogenesis and synaptogenesis in the dentate gyrus of the hippocampus, and reflecting the general observation of 'infantile amnesia' observed on long-term memory tasks but not on short-term memory ability (86).

Our proposal goes farther than the demonstration by Zhang *et al.* (23) that the Hsa21 homologous region on the Mmu17 is a key determinant of cognitive deficits in DS mouse models. We showed here that CBS is a key gene for DS-related phenotypes in mice with the other homologous interval *Cbr3-Fam3b* located on Mmu16, encompassing *Dyrk1a*. We should also consider that in people with DS, both genes are trisomic and thus the recognition memory deficit observed in DS persons and in the complete T21 mouse model (87) certainly depends not only on the interplay between DYRK1A and CBS but also on interaction with other Hsa21 genes that may affect different pathways or different parts of the brain.

The molecular mechanisms involved in *Cbs-Dyr*k1a genetic interaction have been investigated through a quantitative proteomic approach. Although limited due to the complexity of the hippocampus, the results highlight protein network interactions between the two trisomic regions. A total of 208 proteins were found deregulated, corresponding to 148 GO categories and pathways, with 72 specific to Dp1Yah (out of 121) and 9 to *Dyrk1a* transgenic model (out of 32, Supplementary Material, Table S5) and 5 shared between Dp1Yah and Tg(*Dyrk1a*). More interestingly, GO terms such as cortical cytoskeleton or cytoskeletal

protein binding were respectively affected in Dp1Yah and in the Tg(Dyrk1a) but were restored in the double transgenic animals, uncovering somehow the nature of the pathways controlled by the epistatic interaction between CBS and DYRK1A overdosage. DYRK1A is mainly found associated with the actin cytoskeleton modulation (88). CBS is the major enzyme involved in H_2S production in the central nervous system (67). Interestingly, an increase of H_2S activates RAC1 leading to the rearrangement of the actin cytoskeleton during endothelial cell migration (89). Thus, a simple hypothesis would be that the overdosage of CBS may lead to increased H_2S production and further activation of RAC1 with effect on actin cytoskeleton rearrangement, a key mechanism involved in synaptic transmission. Remarkably, DYRK1A interacts with p120-catenin-Kaiso and can then modulate Rac1 (90). Thus, one working hypothesis is based on CBS and DYRK1A pathways connected through RAC1.

DYRK1A is the main driver of defects in DS mouse models for the homologous region to Hsa21 located on Mmu16 (55). Based on a previous study performed in DS models for the Mmu16 homologous region (91), DYRK1A has been selected as a drug target. As reported previously, treatment with epigallocatechin-3-gallate, an inhibitor of DYRK1A kinase activity, can restore some cognitive aspects found altered in people with DS but the gain was limited (16,17). Nevertheless, our results, by adding CBS to the limited number of DS therapeutic targets, may improve the efficiency of DS treatment, in particular by combining multiple therapies to improve the life of DS patients. Finally, an important point to emphasize is that, for DYRK1A as well as for CBS, both loss-of-function mutations and overdosage lead to intellectual deficiencies. This is important to keep in mind when considering a pharmacological intervention that aims at inhibiting one or the other, or both, of these enzymes. Therefore, drug treatment that leads to only a mild inhibition of CBS and/or DYRK1A should be favoured.

Supplementary Material

Supplementary Material is available at *HMG* online.

Acknowledgements

We thank Dr David Patterson for granting access to the 60.4P102D1 transgenic mice, Dr. Nathalie Janel for providing the CBS KO mice, Dr. Henri Blehaut for his initial support on the study and the Fondation Jerome Lejeune for making the transgenic line available and their support. We are grateful to members of the research group, of the proteomic platform of the IGBMC laboratory and of the Mouse Clinical Institute for their help and helpful discussion during the project.

Conflict of Interest statement. None declared.

Funding

French National Centre for Scientific Research; the French National Institute of Health and Medical Research, the Institut Thématique Multiorganisme; Biologie Cellulaire, Développement & Evolution; the University of Strasbourg and the Centre Europeen de Recherche en Biomedecine; the Fondation Jerome Lejeune and the French state funds through the Agence Nationale de la Recherche under the frame programme Investissements d'Avenir labelled [ANR-10-IDEX-0002-02, ANR-10-LABX-0030-INRT, ANR-10-INBS-07 PHENOMIN]. The funders had no role in study design, data collection and analysis, decision to publish or preparation of the manuscript.

References

1. Korbel, J.O., Tirosh-Wagner, T., Urban, A.E., Chen, X.N., Kasowski, M., Dai, L., Grubert, F., Erdman, C., Gao, M.C., Lange, K. *et al.* (2009) The genetic architecture of Down syndrome phenotypes revealed by high-resolution analysis of human segmental trisomies. *Proc. Natl. Acad. Sci. U. S. A.*, **106**, 12031–12036.
2. Lyle, R., Bena, F., Gagos, S., Gehrig, C., Lopez, G., Schinzel, A., Lespinasse, J., Bottani, A., Dahoun, S., Taine, L. *et al.* (2009) Genotype–phenotype correlations in Down syndrome identified by array CGH in 30 cases of partial trisomy and partial monosomy chromosome 21. *Eur. J. Hum. Genet.*, **17**, 454–466.
3. Reeves, R.H., Irving, N.G., Moran, T.H., Wohn, A., Kitt, C., Sisodia, S.S., Schmidt, C., Bronson, R.T. and Davisson, M.T. (1995) A mouse model for Down syndrome exhibits learning and behavior deficits. *Nat. Genet.*, **11**, 177–184.
4. Yu, T., Li, Z.Y., Jia, Z.P., Clapcote, S.J., Liu, C.H., Li, S.M., Asrar, S., Pao, A., Chen, R.Q., Fan, N. *et al.* (2010) A mouse model of Down syndrome trisomic for all human chromosome 21 syntenic regions. *Hum. Mol. Genet.*, **19**, 2780–2791.
5. Duchon, A., Pothion, S., Brault, V., Sharp, A.J., Tybulewicz, V.L.J., Fisher, E.M.C. and Herault, Y. (2011) The telomeric part of the human chromosome 21 from Cstb to Prmt2 is not necessary for the locomotor and short-term memory deficits observed in the Tc1 mouse model of Down syndrome. *Behav. Brain Res.*, **217**, 271–281.
6. Glahn, D.C., Thompson, P.M. and Blangero, J. (2007) Neuroimaging endophenotypes: strategies for finding genes influencing brain structure and function. *Hum. Brain Mapp.*, **28**, 488–501.
7. Brault, V., Duchon, A., Romestaing, C., Sahun, I., Pothion, S., Karout, M., Borel, C., Dembele, D., Bizot, J.C., Messaddeq, N. *et al.* (2015) Opposite phenotypes of muscle strength and locomotor function in mouse models of partial trisomy and monosomy 21 for the proximal Hspa13-App region. *PLoS Genet.*, **11**, e1005062.
8. Herault, Y., Duchon, A., Velot, E., Maréchal, D. and Brault, V. (2012) The in vivo Down syndrome genomic library in mouse. *Prog. Brain Res.*, **197**, 169–197.
9. Jiang, X., Liu, C., Yu, T., Zhang, L., Meng, K., Xing, Z., Belichenko, P.V., Kleschevnikov, A.M., Pao, A., Peresie, J. *et al.* (2015) Genetic dissection of the Down syndrome critical region. *Hum. Mol. Genet.*, **24**, 6540–6551.
10. Hall, J.H., Wiseman, F.K., Fisher, E.M., Tybulewicz, V.L., Harwood, J.L. and Good, M.A. (2016) Tc1 mouse model of trisomy-21 dissociates properties of short- and long-term recognition memory. *Neurobiol. Learn. Mem.*, **130**, 118–128.
11. Lana-Elola, E., Watson-Scales, S., Slender, A., Gibbins, D., Martineau, A., Douglas, C., Mohun, T., Fisher, E.M. and Tybulewicz, V.L.J. (2016) Genetic dissection of Down syndrome-associated congenital heart defects using a new mouse mapping panel. *Elife*, **5**, e11614.
12. Salehi, A., Delcroix, J.D., Belichenko, P.V., Zhan, K., Wu, C., Valletta, J.S., Takimoto-Kimura, R., Kleschevnikov, A.M., Sambamurti, K., Chung, P.P. *et al.* (2006) Increased App expression in a mouse model of Down's syndrome disrupts NGF transport and causes cholinergic neuron degeneration. *Neuron*, **51**, 29–42.

13. García-Cerro, S., Martínez, P., Vidal, V., Corrales, A., Flórez, J., Vidal, R., Rueda, N., Arbonés, M.L. and Martínez-Cué, C. (2014) Overexpression of Dyrk1A is implicated in several cognitive, electrophysiological and neuromorphological alterations found in a mouse model of Down syndrome. *PLoS One*, **9**, e106572.
14. Altafaj, X., Martín, E.D., Ortiz-Abalia, J., Valderrama, A., Lao-Peregrín, C., Dierssen, M. and Fillat, C. (2013) Normalization of Dyrk1A expression by AAV2/1-shDyrk1A attenuates hippocampal-dependent defects in the Ts65Dn mouse model of Down syndrome. *Neurobiol. Dis.*, **52**, 117–127.
15. Guedj, F., Sébrié, C., Rivals, I., Ledru, A., Paly, E., Bizot, J.C., Smith, D., Rubin, E., Gillet, B., Arbones, M. *et al.* (2009) Green tea polyphenols rescue of brain defects induced by overexpression of DYRK1A. *PLoS One*, **4**, e4606.
16. De la Torre, R., De Sola, S., Pons, M., Duchon, A., de Lagran, M.M., Farré, M., Fitó, M., Benejam, B., Langohr, K., Rodriguez, J. *et al.* (2014) Epigallocatechin-3-gallate, a DYRK1A inhibitor, rescues cognitive deficits in Down syndrome mouse models and in humans. *Mol. Nutr. Food Res.*, **58**, 278–288.
17. de la Torre, R., de Sola, S., Hernandez, G., Farré, M., Pujol, J., Rodriguez, J., Espadaler, J.M., Langohr, K., Cuenca-Royo, A., Principe, A. *et al.* (2016) Safety and efficacy of cognitive training plus epigallocatechin-3-gallate in young adults with Down's syndrome (TESDAD): a double-blind, randomised, placebo-controlled, phase 2 trial. *Lancet Neurol.*, **15**, 801–810.
18. Kim, H., Lee, K.S., Kim, A.K., Choi, M., Choi, K., Kang, M., Chi, S.W., Lee, M.S., Lee, J.S., Lee, S.Y. *et al.* (2016) A chemical with proven clinical safety rescues Down-syndrome-related phenotypes in through DYRK1A inhibition. *Dis. Model Mech.*, **9**, 839–848.
19. Nakano-Kobayashi, A., Awaya, T., Kii, I., Sumida, Y., Okuno, Y., Yoshida, S., Sumida, T., Inoue, H., Hosoya, T. and Hagiwara, M. (2017) Prenatal neurogenesis induction therapy normalizes brain structure and function in Down syndrome mice. *Proc. Natl. Acad. Sci. U. S. A.*, **114**, 10268–10273.
20. Neumann, F., Gourdain, S., Albac, C., Dekker, A.D., Bui, L.C., Dairou, J., Schmitz-Afonso, I., Hue, N., Rodrigues-Lima, F., Delabar, J.M. *et al.* (2018) DYRK1A inhibition and cognitive rescue in a Down syndrome mouse model are induced by new fluoro-DANDY derivatives. *Sci. Rep.*, **8**, 2859.
21. Pereira, P.L., Magnol, L., Sahun, I., Brault, V., Duchon, A., Prandini, P., Gruart, A., Bizot, J.C., Chadefaux-Vekemans, B., Deutsch, S. *et al.* (2009) A new mouse model for the trisomy of the Abcg1-U2af1 region reveals the complexity of the combinatorial genetic code of Down syndrome. *Hum. Mol. Genet.*, **18**, 4756–4769.
22. Yu, T., Liu, C.H., Belichenko, P., Clapcote, S.J., Li, S.M., Pao, A.N., Kleschevnikov, A., Bechard, A.R., Asrar, S., Chen, R.Q. *et al.* (2010) Effects of individual segmental trisomies of human chromosome 21 syntenic regions on hippocampal long-term potentiation and cognitive behaviors in mice. *Brain Res.*, **1366**, 162–171.
23. Zhang, L., Meng, K., Jiang, X., Liu, C., Pao, A., Belichenko, P.V., Kleschevnikov, A.M., Josselyn, S., Liang, P., Ye, P. *et al.* (2014) Human chromosome 21 orthologous region on mouse chromosome 17 is a major determinant of Down syndrome-related developmental cognitive deficits. *Hum. Mol. Genet.*, **23**, 578–589.
24. Sahún, I., Marechal, D., Pereira, P.L., Nalesso, V., Gruart, A., Garcia, J.M., Antonarakis, S.E., Dierssen, M. and Herault, Y. (2014) Cognition and hippocampal plasticity in the mouse is altered by monosomy of a genomic region implicated in Down syndrome. *Genetics*, **197**, 899–912.
25. Marechal, D., Lopes Pereira, P., Duchon, A. and Herault, Y. (2015) Dosage of the Abcg1-U2af1 region modifies locomotor and cognitive deficits observed in the Tc1 mouse model of Down syndrome. *PLoS One*, **10**, e0115302.
26. Kimura, H. (2011) Hydrogen sulfide: its production, release and functions. *Amino Acids*, **41**, 113–121.
27. Chen, X., Jhee, K.H. and Kruger, W.D. (2004) Production of the neuromodulator H2S by cystathionine beta-synthase via the condensation of cysteine and homocysteine. *J. Biol. Chem.*, **279**, 52082–52086.
28. Kamat, P.K., Kalani, A. and Tyagi, N. (2015) Role of hydrogen sulfide in brain synaptic remodeling. *Methods Enzymol.*, **555**, 207–229.
29. Watanabe, M., Osada, J., Aratani, Y., Kluckman, K., Reddick, R., Malinow, M.R. and Maeda, N. (1995) Mice deficient in cystathionine beta-synthase: animal models for mild and severe homocyst(e)inemia. *Proc. Natl. Acad. Sci. U. S. A.*, **92**, 1585–1589.
30. Butler, C., Knox, A.J., Bowersox, J., Forbes, S. and Patterson, D. (2006) The production of transgenic mice expressing human cystathionine beta-synthase to study Down syndrome. *Behav. Genet.*, **36**, 429–438.
31. Mantamadiotis, T., Lemberger, T., Bleckmann, S.C., Kern, H., Kretz, O., Martin Villalba, A., Tronche, F., Kellendonk, C., Gau, D., Kapfhammer, J. *et al.* (2002) Disruption of CREB function in brain leads to neurodegeneration. *Nat. Genet.*, **31**, 47–54.
32. Guedj, F., Pereira, P.L., Najas, S., Barallobre, M.J., Chabert, C., Souchet, B., Sebrie, C., Verney, C., Herault, Y., Arbones, M. *et al.* (2012) DYRK1A: a master regulatory protein controlling brain growth. *Neurobiol. Dis.*, **46**, 190–203.
33. Nguyen, T.L., Duchon, A., Manousopoulou, A., Loaëc, N., Villiers, B., Pani, G., Karatas, M., Mechling, A.E., Harsan, L.A., Limanton, E. *et al.* (2018) Correction of cognitive deficits in mouse models of Down syndrome by a pharmacological inhibitor of DYRK1A. *Dis. Model Mech.*, **11**, dmm035634.
34. Mumberg, D., Muller, R. and Funk, M. (1995) Yeast vectors for the controlled expression of heterologous proteins in different genetic backgrounds. *Gene*, **156**, 119–122.
35. Ito, H., Fukuda, Y., Murata, K. and Kimura, A. (1983) Transformation of intact yeast cells treated with alkali cations. *J. Bacteriol.*, **153**, 163–168.
36. Kim, A.K. and Souza-Formigoni, M.L.O. (2010) Disulfiram impairs the development of behavioural sensitization to the stimulant effect of ethanol. *Behav. Brain Res.*, **207**, 441–446.
37. Karp, N.A., Meehan, T.F., Morgan, H., Mason, J.C., Blake, A., Kurbatova, N., Smedley, D., Jacobsen, J., Mott, R.F., Iyer, V. *et al.* (2015) Applying the ARRIVE Guidelines to an In Vivo Database. *PLoS Biol.*, **13**, e1002151.
38. Kilkenny, C., Browne, W.J., Cuthill, I.C., Emerson, M. and Altman, D.G. (2010) Improving bioscience research reporting: the ARRIVE guidelines for reporting animal research. *PLoS Biol.*, **8**, e1000412.
39. Asimakopoulou, A., Panopoulos, P., Chasapis, C.T., Coletta, C., Zhou, Z., Cirino, G., Giannis, A., Szabo, C., Spyroulias, G.A. and Papapetropoulos, A. (2013) Selectivity of commonly used pharmacological inhibitors for cystathionine beta synthase (CBS) and cystathionine gamma lyase (CSE). *Br. J. Pharmacol.*, **169**, 922–932.
40. Thorson, M.K., Van Wagoner, R.M., Harper, M.K., Ireland, C.M., Majtan, T., Kraus, J.P. and Barrios, A.M. (2015) Marine natural products as inhibitors of cystathionine beta-synthase activity. *Bioorg. Med. Chem. Lett.*, **25**, 1064–1066.
41. Thorson, M.K., Majtan, T., Kraus, J.P. and Barrios, A.M. (2013) Identification of cystathionine β-synthase inhibitors using a

hydrogen sulfide selective probe. *Angew. Chem. Int. Ed. Engl.*, **52**, 4641–4644.
42. Zhou, Y., Yu, J., Lei, X., Wu, J., Niu, Q., Zhang, Y., Liu, H., Christen, P., Gehring, H. and Wu, F. (2013) High-throughput tandem-microwell assay identifies inhibitors of the hydrogen sulfide signaling pathway. *Chem. Commun. (Camb)*, **49**, 11782–11784.
43. Jin, S., Chen, Z., Ding, X., Zhao, X., Jiang, X., Tong, Y., Billiard, T.R. and Li, Q. (2016) Cystathionine-beta-synthase inhibition for colon cancer: enhancement of the efficacy of aminooxyacetic acid via the prodrug approach. *Mol. Med.*, **22**, 54–63.
44. Druzhyna, N., Szczesny, B., Olah, G., Módis, K., Asimakopoulou, A., Pavlidou, A., Szoleczky, P., Gerö, D., Yanagi, K., Törö, G. *et al.* (2016) Screening of a composite library of clinically used drugs and well-characterized pharmacological compounds for cystathionine β-synthase inhibition identifies benserazide as a drug potentially suitable for repurposing for the experimental therapy of colon cancer. *Pharmacol. Res.*, **113**, 18–37.
45. Lasserre, J.P., Dautant, A., Aiyar, R.S., Kucharczyk, R., Glatigny, A., Tribouillard-Tanvier, D., Rytka, J., Blondel, M., Skoczen, N., Reynier, P. *et al.* (2015) Yeast as a system for modeling mitochondrial disease mechanisms and discovering therapies. *Dis. Model Mech.*, **8**, 509–526.
46. Voisset, C., Daskalogianni, C., Contesse, M.A., Mazars, A., Arbach, H., Le Cann, M., Soubigou, F., Apcher, S., Fahraeus, R. and Blondel, M. (2014) A yeast-based assay identifies drugs that interfere with Epstein–Barr virus immune evasion. *Dis. Model Mech.*, **7**, 435–444
47. Couplan, E., Aiyar, R.S., Kucharczyk, R., Kabala, A., Ezkurdia, N., Gagneur, J., St Onge, R.P., Salin, B., Soubigou, F., Le Cann, M. *et al.* (2011) A yeast-based assay identifies drugs active against human mitochondrial disorders. *Proc. Natl. Acad. Sci. U. S. A.*, **108**, 11989–11994.
48. Khurana, V., Tardiff, D.F., Chung, C.Y. and Lindquist, S. (2015) Toward stem cell-based phenotypic screens for neurodegenerative diseases. *Nat. Rev. Neurol.*, **11**, 339–350.
49. Bach, S., Talarek, N., Andrieu, T., Vierfond, J.M., Mettey, Y., Galons, H., Dormont, D., Meijer, L., Cullin, C. and Blondel, M. (2003) Isolation of drugs active against mammalian prions using a yeast-based screening assay. *Nat. Biotechnol.*, **21**, 1075–1081.
50. Khurana, V. and Lindquist, S. (2010) Modelling neurodegeneration in Saccharomyces cerevisiae: why cook with baker's yeast? *Nat. Rev. Neurosci.*, **11**, 436–449.
51. Lista, M.J., Martins, R.P., Billant, O., Contesse, M.A., Findakly, S., Pochard, P., Daskalogianni, C., Beauvineau, C., Guetta, C., Jamin, C. *et al.* (2017) Nucleolin directly mediates Epstein–Barr virus immune evasion through binding to G-quadruplexes of EBNA1 mRNA. *Nat. Commun.*, **8**, ncomms16043.
52. Mayfield, J.A., Davies, M.W., Dimster-Denk, D., Pleskac, N., McCarthy, S., Boydston, E.A., Fink, L., Lin, X.X., Narain, A.S., Meighan, M. *et al.* (2012) Surrogate genetics and metabolic profiling for characterization of human disease alleles. *Genetics*, **190**, 1309–1323.
53. Kruger, W.D. and Cox, D.R. (1994) A yeast system for expression of human cystathionine beta-synthase: structural and functional conservation of the human and yeast genes. *Proc. Natl. Acad. Sci. U. S. A.*, **91**, 6614–6618.
54. Aiyar, R.S., Bohnert, M., Duvezin-Caubet, S., Voisset, C., Gagneur, J., Fritsch, E.S., Couplan, E., von der Malsburg, K., Funaya, C., Soubigou, F. *et al.* (2014) Mitochondrial protein sorting as a therapeutic target for ATP synthase disorders. *Nat. Commun.*, **5**, 5585.
55. Duchon, A. and Herault, Y. (2016) DYRK1A, a dosage-sensitive gene involved in neurodevelopmental disorders, is a target for drug development in Down syndrome. *Front. Behav. Neurosci.*, **10**, 104.
56. Hamelet, J., Noll, C., Ripoll, C., Paul, J.L., Janel, N. and Delabar, J.M. (2009) Effect of hyperhomocysteinemia on the protein kinase DYRK1A in liver of mice. *Biochem. Biophys. Res. Commun.*, **378**, 673–677.
57. Planque, C., Dairou, J., Noll, C., Bui, L.C., Ripoll, C., Guedj, F., Delabar, J.M. and Janel, N. (2013) Mice deficient in cystathionine beta synthase display increased Dyrk1A and SAHH activities in brain. *J. Mol. Neurosci.*, **50**, 1–6.
58. Noll, C., Planque, C., Ripoll, C., Guedj, F., Diez, A., Ducros, V., Belin, N., Duchon, A., Paul, J.L., Badel, A. *et al.* (2009) DYRK1A, a novel determinant of the methionine-homocysteine cycle in different mouse models overexpressing this Down-syndrome-associated kinase. *PLoS One*, **4**, e7540.
59. Kwiatkowski, T.J. Jr., Bosco, D.A., Leclerc, A.L., Tamrazian, E., Vanderburg, C.R., Russ, C., Davis, A., Gilchrist, J., Kasarskis, E.J., Munsat, T. *et al.* (2009) Mutations in the FUS/TLS gene on chromosome 16 cause familial amyotrophic lateral sclerosis. *Science*, **323**, 1205–1208.
60. Vance, C., Rogelj, B., Hortobagyi, T., De Vos, K.J., Nishimura, A.L., Sreedharan, J., Hu, X., Smith, B., Ruddy, D., Wright, P. *et al.* (2009) Mutations in FUS, an RNA processing protein, cause familial amyotrophic lateral sclerosis type 6. *Science*, **323**, 1208–1211.
61. Polymeropoulos, M.H., Lavedan, C., Leroy, E., Ide, S.E., Dehejia, A., Dutra, A., Pike, B., Root, H., Rubenstein, J., Boyer, R. *et al.* (1997) Mutation in the alpha-synuclein gene identified in families with Parkinson's disease. *Science*, **276**, 2045–2047.
62. Spillantini, M.G., Schmidt, M.L., Lee, V.M.Y., Trojanowski, J.Q., Jakes, R. and Goedert, M. (1997) Alpha-synuclein in Lewy bodies. *Nature*, **388**, 839–840.
63. Sorensen, J.B., Nagy, G., Varoqueaux, F., Nehring, R.B., Brose, N., Wilson, M.C. and Neher, E. (2003) Differential control of the releasable vesicle pools by SNAP-25 splice variants and SNAP-23. *Cell*, **114**, 75–86.
64. McMahon, H.T. and Sudhof, T.C. (1995) Synaptic core complex of synaptobrevin, syntaxin, and SNAP25 forms high-affinity alpha-SNAP binding site. *J. Biol. Chem.*, **270**, 2213–2217.
65. Zhou, Q., Zhou, P., Wang, A.L., Wu, D., Zhao, M., Südhof, T.C. and Brunger, A.T. (2017) The primed SNARE-complexin-synaptotagmin complex for neuronal exocytosis. *Nature*, **548**, 420–425.
66. Régnier, V., Billard, J.M., Gupta, S., Potier, B., Woerner, S., Paly, E., Ledru, A., David, S., Luilier, S., Bizot, J.C. *et al.* (2012) Brain phenotype of transgenic mice overexpressing cystathionine β-synthase. *PLoS One*, **7**, e29056.
67. Kimura, H. (2002) Hydrogen sulfide as a neuromodulator. *Mol. Neurobiol.*, **26**, 13–19.
68. Kimura, H. (2000) Hydrogen sulfide induces cyclic AMP and modulates the NMDA receptor. *Biochem. Biophys. Res. Commun.*, **267**, 129–133.
69. Hu, L.F., Lu, M., Hon Wong, P.T. and Bian, J.S. (2011) Hydrogen sulfide: neurophysiology and neuropathology. *Antioxid. Redox Signal.*, **15**, 405–419.
70. Johansson, B. (1992) A review of the pharmacokinetics and pharmacodynamics of disulfiram and its metabolites. *Acta Psychiatr. Scand. Suppl.*, **369**, 15–26.

71. Barth, K.S. and Malcolm, R.J. (2010) Disulfiram: an old therapeutic with new applications. *CNS Neurol. Disord. Drug Targets*, **9**, 5–12.
72. Delabar, J.M., Latour, A., Noll, C., Renon, M., Salameh, S., Paul, J.L., Arbones, M., Movassat, J. and Janel, N. (2014) One-carbon cycle alterations induced by Dyrk1a dosage. *Mol. Genet. Metab. Rep.*, **1**, 487–492.
73. Antunes, M. and Biala, G. (2012) The novel object recognition memory: neurobiology, test procedure, and its modifications. *Cogn. Process.*, **13**, 93–110.
74. Clark, R.E., Zola, S.M. and Squire, L.R. (2000) Impaired recognition memory in rats after damage to the hippocampus. *J. Neurosci.*, **20**, 8853–8860.
75. Clarke, J.R., Cammarota, M., Gruart, A., Izquierdo, I. and Delgado-Garcia, J.M. (2010) Plastic modifications induced by object recognition memory processing. *Proc. Natl. Acad. Sci. U. S. A.*, **107**, 2652–2657.
76. Reger, M.L., Hovda, D.A. and Giza, C.C. (2009) Ontogeny of rat recognition memory measured by the novel object recognition task. *Dev. Psychobiol.*, **51**, 672–678.
77. Stackman, R.W., Cohen, S.J., Lora, J.C. and Rios, L.M. (2016) Temporary inactivation reveals that the CA1 region of the mouse dorsal hippocampus plays an equivalent role in the retrieval of long-term object memory and spatial memory. *Neurobiol. Learn. Mem.*, **133**, 118–128.
78. Warburton, E.C. and Brown, M.W. (2015) Neural circuitry for rat recognition memory. *Behav. Brain Res.*, **285**, 131–139.
79. Benchenane, K., Peyrache, A., Khamassi, M., Tierney, P.L., Gioanni, Y., Battaglia, F.P. and Wiener, S.I. (2010) Coherent theta oscillations and reorganization of spike timing in the hippocampal–prefrontal network upon learning. *Neuron*, **66**, 921–936.
80. Wei, J., Bai, W.W., Liu, T.T. and Tian, X. (2015) Functional connectivity changes during a working memory task in rat via NMF analysis. *Front. Behav. Neurosci.*, **9**, 2.
81. Lin, J.D., Wu, P.H., Tarr, P.T., Lindenberg, K.S., St-Pierre, J., Zhang, C.Y., Mootha, V.K., Jager, S., Vianna, C.R., Reznick, R.M. *et al.* (2004) Defects in adaptive energy metabolism with CNS-linked hyperactivity in PGC-1 alpha null mice. *Cell*, **119**, 121.
82. Vallone, D., Picetti, R. and Borrelli, E. (2000) Structure and function of dopamine receptors. *Neurosci. Biobehav. Rev.*, **24**, 125–132.
83. Bymaster, F.P., Katner, J.S., Nelson, D.L., Hemrick-Luecke, S.K., Threlkeld, P.G., Heiligenstein, J.H., Morin, S.M., Gehlert, D.R. and Perry, K.W. (2002) Atomoxetine increases extracellular levels of norepinephrine and dopamine in prefrontal cortex of rat: a potential mechanism for efficacy in attention deficit/hyperactivity disorder. *Neuropsychopharmacology*, **27**, 699–711.
84. Cador, M., Robbins, T.W. and Everitt, B.J. (1989) Involvement of the amygdala in stimulus-reward associations: interaction with the ventral striatum. *Neuroscience*, **30**, 77–86.
85. Anderson, M.J., Barnes, G.W., Briggs, J.F., Ashton, K.M., Moody, E.W., Joynes, R.L. and Riccio, D.C. (2004) Effects of ontogeny on performance of rats in a novel object-recognition task. *Psychol. Rep.*, **94**, 437–443.
86. Rudy, J.W. and Morledge, P. (1994) Ontogeny of contextual fear conditioning in rats: implications for consolidation, infantile amnesia, and hippocampal system function. *Behav. Neurosci.*, **108**, 227–234.
87. Belichenko, P.V., Kleschevnikov, A.M., Becker, A., Wagner, G.E., Lysenko, L.V., Yu, Y.E. and Mobley, W.C. (2015) Down syndrome cognitive phenotypes modeled in mice trisomic for all HSA 21 homologues. *Plos One*, **10**, e0134861.
88. Park, J., Sung, J.Y., Song, W.J., Chang, S. and Chung, K.C. (2012) Dyrk1A negatively regulates the actin cytoskeleton through threonine phosphorylation of N-WASP. *J. Cell Sci.*, **125**, 67–80.
89. Zhang, L.J., Tao, B.B., Wang, M.J., Jin, H.M. and Zhu, Y.C. (2012) PI3K p110α isoform-dependent Rho GTPase Rac1 activation mediates H2S-promoted endothelial cell migration via actin cytoskeleton reorganization. *PLoS One*, **7**, e44590.
90. Hong, J.Y., Park, J.I., Lee, M., Muñoz, W.A., Miller, R.K., Ji, H., Gu, D., Ezan, J., Sokol, S.Y. and McCrea, P.D. (2012) Down's-syndrome-related kinase Dyrk1A modulates the p120-catenin-Kaiso trajectory of the Wnt signaling pathway. *J. Cell Sci.*, **125**, 561–569.
91. Herault, Y., Delabar, J.M., Fisher, E.M.C., Tybulewicz, V.L.J., Yu, E. and Brault, V. (2017) Rodent models in Down syndrome research: impact and future opportunities. *Dis. Model Mech.*, **10**, 1165–1186.